



Review

# Textile Materials for Wireless Energy Harvesting

Yusuke Yamada

Yamada Shoten, Osaka 556-0001, Japan; ymukai@ncsu.edu

**Abstract:** Wireless energy harvesting, a technique to generate direct current (DC) electricity from ambient wireless signals, has recently been featured as a potential solution to reduce the battery size, extend the battery life, or replace batteries altogether for wearable electronics. Unlike other energy harvesting techniques, wireless energy harvesting has a prominent advantage of ceaseless availability of ambient signals, but the common form of technology involves a major challenge of limited output power because of a relatively low ambient energy density. Moreover, the archetypal wireless energy harvesters are made of printed circuit boards (PCBs), which are rigid, bulky, and heavy, and hence they are not eminently suitable for body-worn applications from both aesthetic and comfort points of view. In order to overcome these limitations, textile-based wireless energy harvesting architectures have been proposed in the past decade. Being made of textile materials, this new class of harvesters can be seamlessly integrated into clothing in inherently aesthetic and comfortable forms. In addition, since clothing offers a large surface area, multiple harvesting units can be deployed to enhance the output power. In view of these unique and irreplaceable benefits, this paper reviews key recent progress in textile-based wireless energy harvesting strategies for powering body-worn electronics. Comparisons with other power harvesting technologies, historical development, fundamental principles of operation and techniques for fabricating textile-based wireless power harvesters are first recapitulated, followed by a review on the principal advantages, challenges, and opportunities. It is one of the purposes of this paper to peruse the current state-of-the-art and build a scientific knowledge base to aid further advancement of power solutions for wearable electronics.



**Citation:** Yamada, Y. Textile Materials for Wireless Energy Harvesting. *Electron. Mater.* **2022**, *3*, 301–331. <https://doi.org/10.3390/electronicmat3040026>

Academic Editor: Wojciech Pisula

Received: 31 August 2022

Accepted: 26 September 2022

Published: 8 October 2022

**Publisher's Note:** MDPI stays neutral with regard to jurisdictional claims in published maps and institutional affiliations.



**Copyright:** © 2022 by the author. Licensee MDPI, Basel, Switzerland. This article is an open access article distributed under the terms and conditions of the Creative Commons Attribution (CC BY) license (<https://creativecommons.org/licenses/by/4.0/>).

**Keywords:** wireless power harvesting; textile-based energy solution; self-sustainable wearable electronics; high-frequency circuit design; electrical and dielectric properties

## 1. Introduction

With ever-increasing interest in anytime anywhere access to various electronic functionalities, electronic textiles (e-textiles) have been featured in recent research. Having both functions as electronics and comfortable apparel, textile-based electronics have been advocated to remove the technical hurdle for long-term detection and sensing, data analysis and transmission for various healthcare [1–3], military [4], space [5] and entertainment [6] applications.

One major challenge with the current e-textile technology is power supply [7]. Most e-textile products are powered by conventional rechargeable or disposable batteries that are heavy and bulky [8]. It has been pointed out, for instance, that batteries could account for nearly 20% of the carry-on load for U.S. soldiers on mission [8,9]. Although efforts have been made to develop lightweight, flexible, and small form-factor power storage devices [10], these substitutes have not yet reached the capacity of conventional ones [8].

As an alternative approach, ambient energy harvesting has been spotlighted. Ambient energy harvesting is a technique to generate direct current (DC) electricity from ambient energy. Several energy sources have been identified for ambient energy harvesting, including wireless energy from telecommunication (e.g., mobile, satellite and Wi-Fi) signals [11–13], light energy from the sun and artificial light [14,15], kinetic energy from

vibrations, body motions and airflow [16–18], and thermal energy from body and waste heat [19–21]. Although each source has reasons to support and oppose [22], wireless energy has a prominent advantage of ceaseless availability—wireless signals are almost always available regardless of the location and time [12]. In addition, it has recently been demonstrated that wireless energy harvesting units can be produced in inherently aesthetic and comfortable forms by using textile materials, making this option perfectly viable for powering body-worn electronics that are expected to function in both indoor and outdoor settings without interruption [23–27]. Moreover, multiple textile-based energy harvesters can be incorporated into clothing, which offers a large surface area for such integration, to enhance the output power. To date, various textile-based wireless energy harvesters have been proposed for these reasons.

Given this context, this paper reviews the textile-based wireless energy harvesting technology for powering wearable electronics with respect to the early concept and fundamental principles, advantages and challenges of using textile materials, fabrication techniques, recent research mainstream, and future perspectives. It is one of the purposes of this paper to summarize the current state-of-the-art and build a scientific knowledge base for this rapidly expanding realm of research.

## 2. Comparison of Various Ambient Energy Harvesting Techniques for Powering Wearable Electronics

Light, kinetic, thermal, and wireless energies are the four major categories of ambient sources from which electricity can be harvested (Figure 1). Light energy is one of the most popular ambient energy sources and can be converted into electricity by a photovoltaic cell. Photovoltaic cells have been successfully rendered into textile forms for wearable applications, and a high power output was proven to be attainable in areas where there is consistent sunshine (Figure 2 and Table 1) [28–30]. However, during dark hours or in indoor environment, the output power is considerably reduced [31].

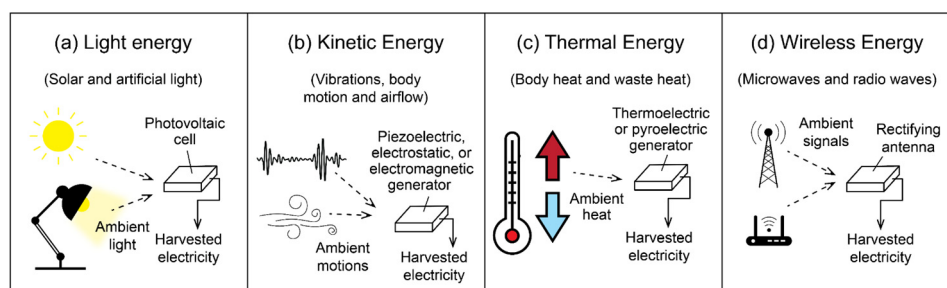


**Figure 1.** Various ambient sources for energy harvesting applications: (a) microwaves and radio waves for wireless energy harvesting, (b) solar and artificial light for light energy harvesting, (c) vibrations, body motion and airflow for kinetic energy harvesting, and (d) body and waste heat for thermal energy harvesting.

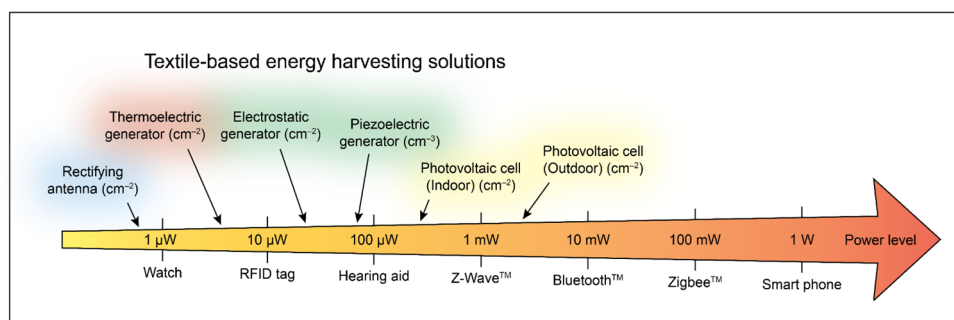


**Figure 2.** Energy harvesting performance of textile-based solutions [32–41] and power consumption of common electronics [42–47].

**Table 1.** Ambient energy sources and harvesters for wearable applications.

Energy Category	Ambient Energy Source	Ambient Power Density	Harvesting Mechanism	Non-Textile Solution		Textile-Based Solution	
				Harvestable Power Density	Efficiency (%)	Harvestable Power Density	Efficiency (%)
Light energy	Outdoor (irect sun light)	0.1 W/cm <sup>2</sup> [48]	Photovoltaic cell	15 mW/cm <sup>2</sup> [14]	19.44 [49]	2.15–4.6 mW/cm <sup>2</sup> [32–34]	0.6–4.6 [29,30,33]
	Indoor light	0.01–1.8 mW/cm <sup>2</sup> [14,33,50]		0.22 mW/cm <sup>2</sup> [15]		0.14 mW/cm <sup>2</sup> [33]	
Kinetic energy	Body motion	–	Piezoelectric generator	7.8–81.25 $\mu$ W/cm <sup>3</sup> [51,52]	0.5–50 [53,54]	2–87 $\mu$ W/cm <sup>3</sup> [35,36]	27–40 [35]
			Electrostatic generator	50–193.6 $\mu$ W/cm <sup>2</sup> [55,56]		1.56–46.6 $\mu$ W/cm <sup>2</sup> [37–39]	
Thermal Energy	Body heat (at rest)	1–10 mW/cm <sup>2</sup> [20,59]	Thermoelectric generator	15.8–97.6 $\mu$ W/cm <sup>2</sup> [20,60,61]	5–24 [62,63]	5.15–7 $\mu$ W/cm <sup>2</sup> [40,41]	
Wireless energy	Radiofrequency and microwave radiation	0.00018–1 $\mu$ W/cm <sup>2</sup> [64,65]	Rectenna	0.08 nW/cm <sup>2</sup> –1 $\mu$ W/cm <sup>2</sup> [66]	30–88 [66]	–	28.7–50 [24,67,68]

Kinetic energies in the form of vibrations, body motions, and airflow are the second category of ambient energy and can be converted into electricity by piezoelectric, electrostatic, or electromagnetic generators. Although kinetic energy harvesting has been widely examined for wearable applications [69], one of the major disadvantages of kinetic energy is discontinuous availability—kinetic energy from human motions is often intermittent and unpredictable [70].

Thermal energy, such as body or waste heat, can also be transformed into electricity, and a thermoelectric material is generally used to achieve energy conversion. Some of the commonly investigated thermoelectric materials are bismuth telluride [71], antimony telluride [72], and copper sulfides [73–76], but because of their bulkiness and brittleness, these substances are not ideal for wearable applications [8,76–78]. In view of these limitations, textile-based flexible thermoelectric generators made of poly(3,4-ethylenedioxythiophene):poly(styrene sulfonate) (PEDOT:PSS) have recently been proposed for on-body harvesting applications [8,77,79]. Yet, thermal energy harvesting has a major drawback of low efficiency—an efficient thermoelectric material needs to have both low electrical resistivity and low thermal conductivity, but such combinations are hardly achievable [80,81]. In addition, because the amount of harvestable energy depends on the temperature difference between the human body and ambient temperature, the power output is critically affected by the climate [82].

The last category of ambient source is wireless energy, which is electromagnetic radiation from telecommunication base stations (e.g., television and radio towers, cell sites, satellite stations and Wi-Fi routers), wireless mobile devices (e.g., smart phones, personal data assistants, and tablet and laptop computers), or any other wireless systems [82,83]. Unlike solar, kinetic, and thermal energies, whose availability depends on the location, time, climate, and/or other relevant factors, wireless signals are ceaselessly available in present times [12]. In wireless energy harvesting, ambient signals are converted into electricity by a rectifying antenna (or rectenna) that can be produced in an inherently aesthetic and comfortable form from textile materials; therefore, wireless energy harvesting is a propitious solution to continuously power body-worn electronics [23–27].

There is, however, a major challenge in wireless energy harvesting. Compared with the other ambient sources, the available ambient power density is much lower for wireless signals (Table 1) [66]. Nevertheless, wireless energy harvesting has practical significance because of its high energy conversion efficiency (Table 1). In addition, if a higher output is required, multiple rectennas could be incorporated into clothing to support more power-demanding electronics [24,84].

### 3. Major Milestones in Wireless Power Transfer and Wireless Energy Harvesting

As summarized in Figure 3, the history of wireless power transmission, an essential phenomenon in wireless energy harvesting, could date back to 1873, when James Clerk Maxwell unified the theories of light and electromagnetism and predicted the transmission of electrical energy in free space [85]. This prediction was, for the first time, attested in 1899 by Nikola Tesla, who lighted a fluorescent lamp from a distance of 25 miles by using a low-frequency electrical resonant transformer circuit, commonly known as Tesla coil [86]. Although the Tesla's innovation never found an applicable route to its commercialization [87], the concept of wireless power transmission has led to various consequential applications—it requires no physical element between the source of energy and the point of consumption, and the energy can be transferred at the speed of light with almost neglectable attenuation losses [85].

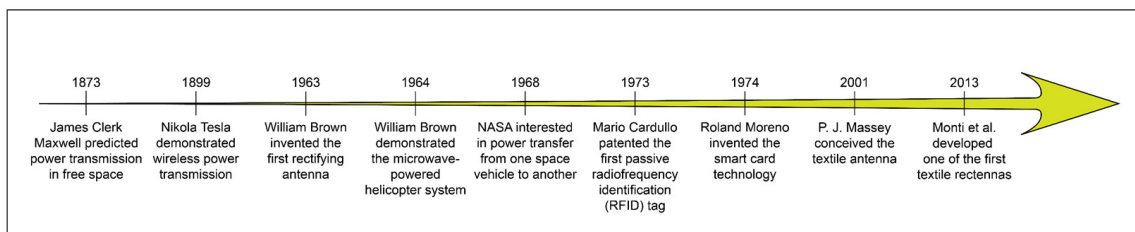


**Figure 3.** Major milestones in wireless power transfer and wireless energy harvesting [85,88–93].

One of the most revolutionary inventions that are based on wireless power transmission is a rectenna. A rectenna is an antenna integrated with a rectifying circuit to absorb (i.e., receive) wireless signals and convert them into DC electricity [85]. The rectenna was conceived by William Brown in 1963, and a year later, a rectenna-based, microwave-powered helicopter system was developed for demonstration of wireless power transfer on television [85,90]. As illustrated in Figure 4, the helicopter system was transiently charged by the embedded rectenna that absorbed microwave energy emitted from the power source (reflector antenna) placed on the ground. This system could be seen, in one view, as one of the earliest examples of wireless energy harvesting.

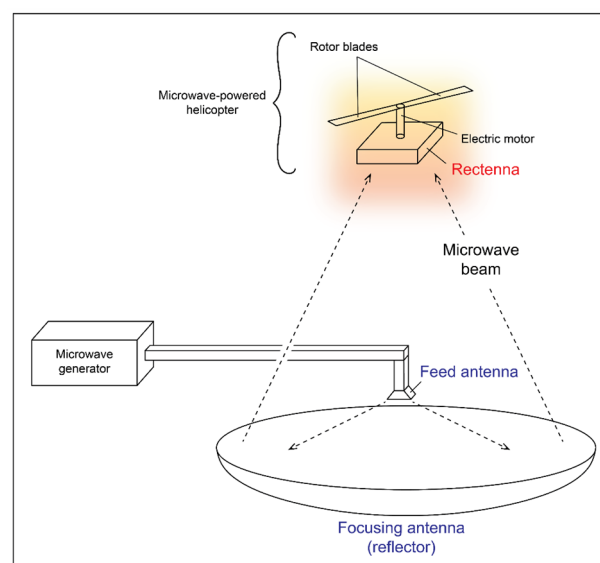


**Figure 4.** Schematic illustration of the microwave-powered helicopter system televised in 1964, redrawn from [85] (p. 6).



Although the initial motivation for developing a rectenna was to power a high-altitude atmospheric platform by a focused microwave beam under the Raytheon Company and the United States Air Force sponsorship, the rectenna technology has soon led to various industrially important investigations and applications [90]. Those include the power transfer exploration for space vehicles by the National Aeronautics and Space Administration (NASA) in 1968 [90], development of radiofrequency identification (RFID) tag by Mario Cardullo in 1973 [93,94], and invention of smart card technology by Roland Moreno in 1974 [95,96]. Currently, various rectenna-based wireless power transmission techniques are used for charging smartphones and smartwatches [97], electric vehicles [98–100], and medical implants [101].

As a potential method to power textile-based electronics, the rectenna technology has also been spotlighted in the textile industry. In 2001, P.J. Massey developed the first textile-based antenna, which was constructed by combining a copper-plated ripstop nylon fabric as a conductor and a breathable foam as a dielectric spacer [88]. Although this very first example had a considerable thickness (i.e., the breathable foam alone had a thickness of 12.5 mm), significantly thin designs were soon devised [102–105]. One of the first textile-based rectennas was reported by Monti et al. in 2013 and was made of a copper-plated nylon non-woven fabric as a conductor and pile and denim fabrics as dielectric substrate [24,25,67]. The rectification circuit was on the denim layer attached to the ground plane of the antenna, and the energy conversion efficiency was as high as 50% at the frequency of 876 MHz [67].

Since then, it has been well-documented that textile-based rectennas could be an ideal candidate for powering body-worn electronics because of their innately wearable form factors [23–26], but equally importantly, textile materials could have a relatively low electrical permittivity owing to their highly porous nature, and therefore, the use of textile materials has great potential in ameliorating the gain, efficiency and frequency bandwidth of the conventional materials such as printed circuit boards (PCBs) [106–109]. The latter aspect is exceedingly invaluable for ambient wireless energy harvesting applications, where available energy is limited and enhancement of the energy conversion efficiency is of paramount importance [24]. To date, myriads of textile-based designs have been proposed for these reasons.

## 4. Principles of Wireless Energy Harvesting

### 4.1. Antennas

The principal components in wireless energy harvesting are drawn in Figure 5 and are a receiving antenna, an impedance matching circuit, a rectifier (or a voltage multiplier), and a load (or a power management unit). A receiving antenna is the unit that receives ambient wireless signals and converts them into alternating current (AC) electricity as depicted in Figure 6. Receiving antennas can generally be classified into wire, traveling wave, log-periodic, microstrip, aperture, and reflector antennas (Figure 7) [110], and the antenna performance, form factors and design strategies or rules are primarily dependent on the antenna type. For instance, wire antennas can be designed in a simple linear (dipole, folded dipole, sleeve, and monopole) or curved (loop) geometry with dimensions directly related to the wavelength ( $\lambda$ ), although there are several exceptions [111]. The radiation patterns of wire antennas are typically omnidirectional and hence are commonly used to receive broadcast and cellular signals. This class of antennas was, for instance, employed by Nguyen et al. to develop a wireless energy harvesting necklace to power a fitness monitor pendant in stand-by mode [112]. In their design, a dipole antenna was bent to form a U-shape to be part of the necklace, and good comfort and aesthetic appearance were achieved in addition to the required energy harvesting performance [112].

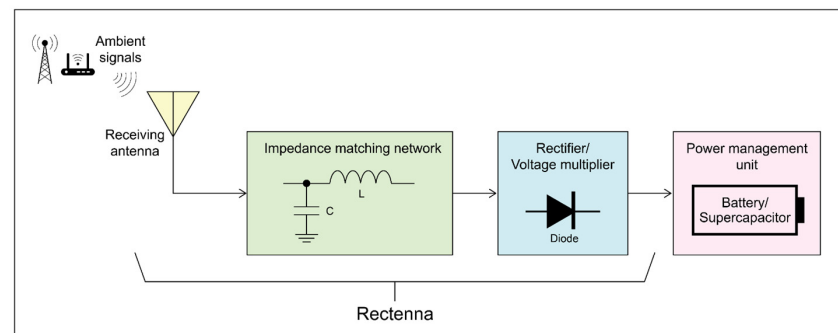


**Figure 5.** Essential energy extraction and storage components in wireless energy harvesting, redrawn from [113] (p. 17233) and [12] (p. 2).

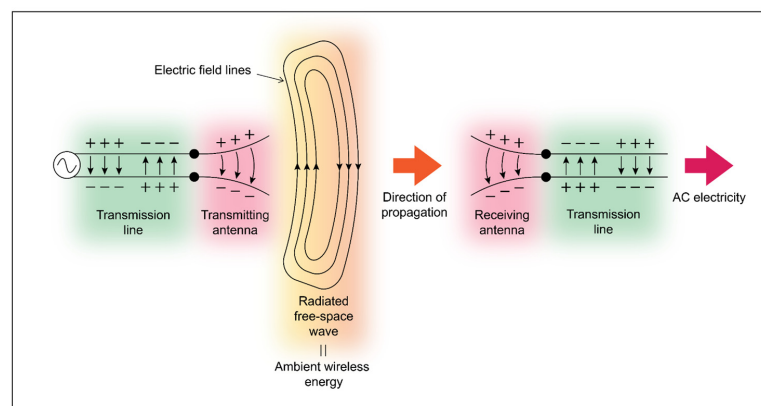


**Figure 6.** Schematic illustration of antenna transmission and reception, redrawn from [110] (p. 25) and [114] (p. 11).

Antenna type	Subtype	Basic geometry	Antenna type	Subtype	Basic geometry
Wire antennas	Dipole antennas		Log-periodic antennas	Bow-tie antennas	
	Folded dipole antennas			Log-periodic array antenna	
	Sleeve antennas		Microstrip antennas	Patch antennas	
	Monopole antennas			Planar inverted-F antennas	
	Loop antennas		Aperture antennas	Horn antennas	
Traveling wave antennas	Spiral antennas			Slot antennas	
	Helical antennas			Vivaldi antennas	
	Yagi-Uda antennas		Reflector antennas	Parabolic antennas	
				Corner reflector antenna	

**Figure 7.** Classification and geometry of basic antennas, redrawn from [110] (pp. 26–30), [115] (p. 3) and [88] (p. 344).

Traveling wave antennas such as spiral, helical, and Yagi-Uda antennas are based on a traveling wave on a guided structure as the main radiating mechanism [116]. Although some of these antennas can operate in the normal (omnidirectional) mode, they are usually employed as a directional antenna for better efficiency. Among various traveling wave antennas, spiral antennas have been frequently investigated in wearable wireless energy harvesting research for their low-profile planar structure and wide bandwidth [117,118]. In addition, the radiation characteristics of spiral antennas can be easily adjusted by changing the circular radius, number of turns, spacing between turns, and width of the spiral arm, making this class of antennas a great option [118].

Log-periodic antennas such as bowtie and log-periodic array antennas are wide-band antennas, which exhibit essentially constant characteristics over a broad frequency range [114,119,120]. In addition, they can be produced in planar forms [121–124], and hence, log-periodic antennas are suitable for wireless energy harvesting applications that require reception of broadband frequencies, although characterized by a relatively low gain [125–127].

Microstrip antennas are planar antennas consisting of a conductive layer mounted on a grounded substrate, and patch antennas and planar inverted-F antennas are grouped into this category. Although microstrip antennas have several drawbacks such as narrow bandwidth, low power handling capabilities, high dielectric and conductor losses, they are the most commonly used antennas in wireless energy harvesting as they are lightweight, low-cost, high-efficiency, easy to produce from a PCB [128–130]. It is also favorable for rectenna applications that the ground plane layer of the patch antenna could eliminate the possibility of undesirable interference between the antenna and human body [131,132]. The dimensions of the patch antennas can be easily determined from the wavelength and the dielectric properties of the substrate by simple analytical formulas [114,133,134], but for a better accuracy, an electromagnetic simulator is often used [135].

Aperture antennas contain some sort of opening through which wireless signals are received or transmitted, and the representative examples are horn, slot, and Vivaldi antennas [114]. Among these antennas, slot and Vivaldi antennas have been studied for wearable wireless energy harvesting applications as they can be produced in compact, planar shape [136–141]. On the other hand, horn antennas are usually not considered for on-body applications because of their heavy weight and bulkiness—they are mostly employed for spacecraft and aircraft applications with the opening (aperture) covered by a dielectric material for minimization of aerodynamic impact and protection from environmental conditions [114].

Reflector antennas such as parabolic and corner reflector antennas are antennas that uses a reflector to direct wireless signals to the receiver (feed antenna) in its focal point. Hence the major advantage is their high gain [110], which is ideal for radio astronomy, satellite tracking, and deep-space communication applications [114]. On the other hand, because the reflector and feed antenna are placed physically apart, the antenna size is usually large and opted out for wearable applications [114].

#### 4.2. Impedance Matching Networks

The second essential element in wireless energy harvesting is the impedance matching circuit, which ensures that the power received by the antenna is fully delivered to the rectifying unit without reflection [142]. For wireless energy harvesting applications, design of an impedance matching network involves complications. This is because the input impedance of the rectifier depends not only on the frequency of the input signal but also on its power level, which is fairly complex to predict as the instantaneous wireless signal available in the environment is constantly changing [24]. Consequently, designing a highly efficient impedance matching networks is of great challenge particularly for wideband applications [142], and even elimination of matching circuit has been suggested [142,143].

While various impedance matching techniques have been devised, three of the most common structures for wireless energy harvesting applications are the quarter-wave trans-

former, tuning stub, and lumped element networks (Figure 8). The quarter-wave transformer network is an intermediate section of length  $l$  ( $=\lambda/4$ ) that can be placed between two systems of different impedances to match the impedance (Figure 9) [82]. Although this type of network can only match the real part of the impedance at a single frequency, they have been commonly employed for the simplicity in design and fabrication [82]. The characteristic impedance of a quarter-wave transformer ( $Z_Q$ ) required to match the input transmission line impedance ( $Z_0$ ) and the load impedance ( $Z_L$ ) is given by [144]:

$$Z_Q = \sqrt{Z_0 Z_L} \quad (1)$$

The width of the trace ( $W_T$ ) can then be determined by plugging the value of  $Z_Q$  into Equation (2) and solving it for  $W_T$  [114]:

$$Z_Q = \begin{cases} \frac{60}{\sqrt{\epsilon'_{r,eff}}} \ln\left(\frac{8h_S}{W_T} + \frac{W_T}{4h_S}\right) & \text{for } \frac{W_T}{h_S} \leq 1 \\ \frac{120\pi}{\sqrt{\epsilon'_{r,eff}} \left[ \frac{W_T}{h_S} + 1.393 + 0.667 \ln\left(\frac{W_T}{h_S} + 1.444\right) \right]} & \text{for } \frac{W_T}{h_S} > 1 \end{cases} \quad (2)$$

where  $\epsilon'_{r,eff}$  and  $h_S$  are the effective dielectric constant and thickness of the substrate, respectively. For  $W_T/h_S \gg 1$ ,  $\epsilon'_{r,eff}$  can be calculated by [114]:

$$\epsilon'_{r,eff} = \frac{\epsilon'_r + 1}{2} + \frac{\epsilon'_r - 1}{2} \left(1 + \frac{12h_S}{W_T}\right)^{-\frac{1}{2}} \quad (3)$$

where  $\epsilon'_r$  is the dielectric constant of the substrate.

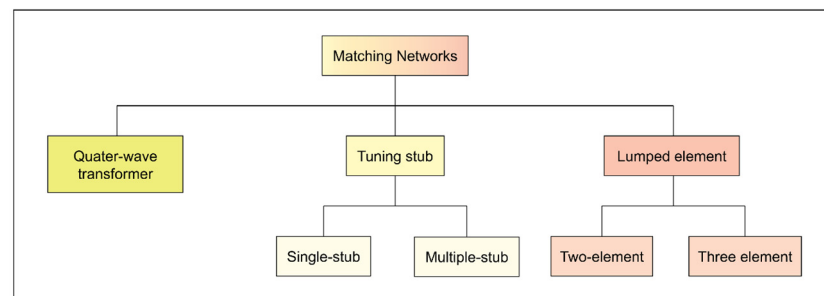


**Figure 8.** Matching network taxonomy for wireless energy harvesting applications, redrawn from [82] (p. 76).

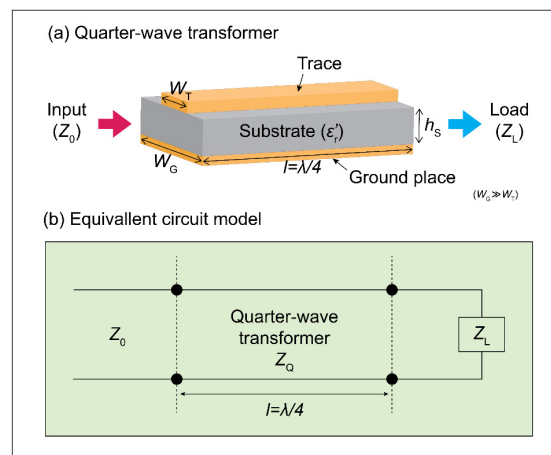


**Figure 9.** Schematic illustration of (a) a quarter-wave transformer and (b) its equivalent circuit model, redrawn from [145] (p. 36) and [144] (p. 247).

The stub tuning network is an impedance matching technique based on another transmission line connected to the main transmission line, and some of the topologies are shown in Figure 10 [146]. Among these configurations, open-circuit shunt stubs are predominantly used in wireless energy harvesting applications as they are the simplest to fabricate [144]. In order to determine the appropriate position and dimensions of a tuning stub, analytical formulas can be used. For the position of the tuning stub, its distance from the load ( $d$ ) is chosen so as to cancel the real part of the load impedance (or admittance) and hence can be calculated by [144]:

$$d = \begin{cases} \frac{\lambda}{2\pi} \tan^{-1} A & \text{for } A \geq 0 \\ \frac{\lambda}{2\pi} (\pi + \tan^{-1} A) & \text{for } A < 0 \end{cases} \quad (4)$$

where  $A$  is given by [144]:

$$A = \begin{cases} \frac{X_L \pm \sqrt{\frac{R_L [(Z_0 - R_L)^2 + X_L^2]}{Z_0}}}{R_L - Z_0} & \text{for shunt stubs with } R_L \neq Z_0 \\ \frac{-X_L}{2Z_0} & \text{for shunt stubs with } R_L = Z_0 \\ \frac{B_L \pm \sqrt{\frac{G_L [(Y_0 - G_L)^2 + B_L^2]}{Y_0}}}{G_L - Y_0} & \text{for series stubs with } G_L \neq Y_0 \\ \frac{-B_L}{2Y_0} & \text{for series stubs with } G_L = Y_0 \end{cases} \quad (5)$$

where  $R_L$  and  $X_L$  are the real and imaginary parts of the load impedance, respectively;  $G_L$  and  $B_L$  are the real and imaginary parts of the load admittance, respectively; and  $Y_0$  is the input transmission line admittance.

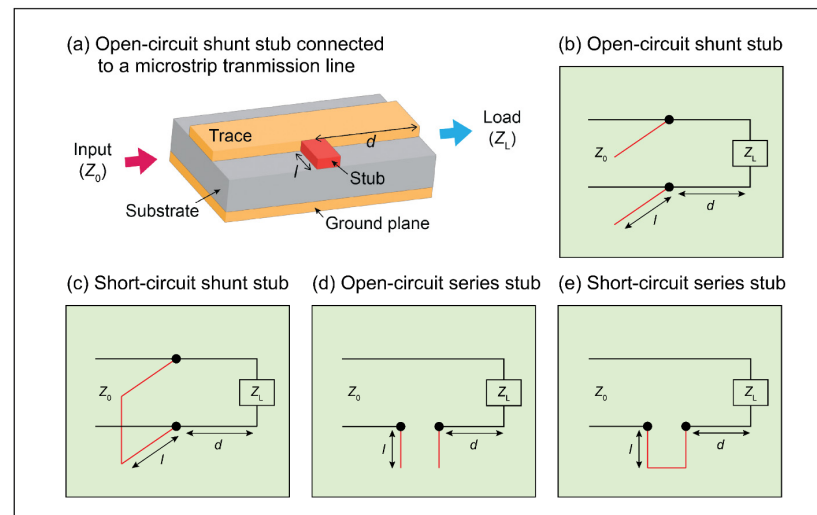


**Figure 10.** Schematic illustration of (a) an open-circuit shunt stub, (b) its equivalent circuit model, and circuit models of (c) short-circuit shunt, (d) open-circuit series, and (e) short-circuit series stubs, redrawn from [146] (pp. 11–12) and [147] (p. 3).

The stub length ( $l$ ), on the other hand, is chosen to introduce a capacitive or inductive reactance (or susceptance) that has the same magnitude but in opposite sign to match the imaginary part [146,148]. Hence, the stub length is given by [144]:



$$l = \begin{cases} \frac{\lambda}{2\pi} \tan^{-1} \left( \frac{B_S}{Y_0} \right) & \text{for an open – circuit shunt stub} \\ \frac{-\lambda}{2\pi} \tan^{-1} \left( \frac{Y_0}{B_S} \right) & \text{for a short – circuit shunt stub} \\ \frac{-\lambda}{2\pi} \tan^{-1} \left( \frac{Z_0}{X_S} \right) & \text{for an open – circuit series stub} \\ \frac{\lambda}{2\pi} \tan^{-1} \left( \frac{X_S}{Z_0} \right) & \text{for a short – circuit series stub} \end{cases} \quad (6)$$

where  $X_S$  and  $B_S$  are the imaginary parts of the stub impedance and admittance, respectively.

Although the stub-based method can match both real and imaginary parts of the impedance [82], a single stub will only achieve a perfect match at one specific frequency. This is because the reactance is a function of the frequency, but such compensation can be only done by changing the physical position ( $d$ ) of the stub [146]. For variable matching circuits, therefore, a second stub is required to provide an additional degree of freedom. More details on the multi-stub strategies are described in [149,150].

Lumped elements can also be used to achieve the impedance matching. Based on the topology, lumped elements can be categorized into L-type,  $\Pi$ -type, and T-type networks (Figure 11). The L-type network, which has a simple architecture that resembles the letter L, usually consists of a series capacitor with a shunt (parallel) inductor (or vice versa) [148]. The function of the shunt component is to transform a larger impedance down to a smaller value equating the real part of the impedances between the source and the load. Thus, the shunt susceptance ( $B$ ) is given by [144]:

$$B = \begin{cases} \frac{X_L \pm \sqrt{\frac{R_L}{Z_0} \sqrt{R_L^2 + X_L^2 - Z_0 R_L}}}{R_L^2 + X_L^2} & \text{for } Z_0 < R_L \\ \pm \frac{\sqrt{\frac{Z_0 - R_L}{R_L}}}{Z_0} & \text{for } Z_0 > R_L \end{cases} \quad (7)$$

On the other hand, the series component cancels out any reactive components by resonating with equal and opposite reactance [151], and accordingly the series reactance is given by [144]:

$$X = \begin{cases} \frac{1}{B} + \frac{X_L Z_0}{R_L} - \frac{Z_0}{B R_L} & \text{for } Z_0 < R_L \\ \pm \sqrt{R_L (Z_0 - R_L)} - X_L & \text{for } Z_0 > R_L \end{cases} \quad (8)$$

Therefore, these two elements of the L-type network together leave the source driving an equal load for the maximum power transfer.

One of the major drawbacks of the L-type network is its inability to control the matching bandwidth. For applications that require a narrow bandwidth such as to match a narrowband antenna, the  $\Pi$ -type or T-type networks can be formed by introducing an additional element [152]. The  $\Pi$ -type network has a configuration resembling the Greek letter  $\Pi$ , whereas the T-type network has a T-like configuration and is a dual of the  $\Pi$ -type network; the third element provides an additional degree of freedom that enables the bandwidth control [151]. However, because of the additional element, the  $\Pi$ -type or T-type networks usually have a higher component loss than the two-element (L-type) network [151].

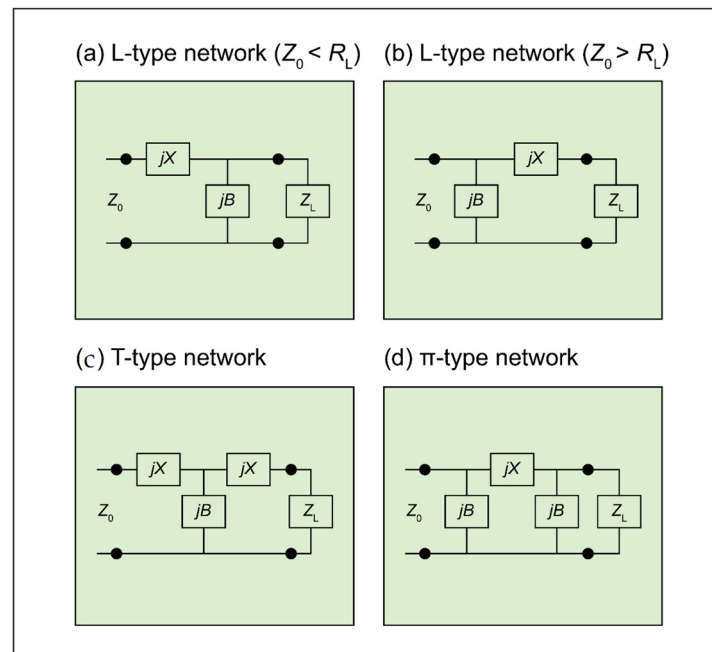


**Figure 11.** Schematic illustration of basic impedance matching networks: (a) L-type ( $Z_0 < R_L$ ), (b) L-type ( $Z_0 > R_L$ ), (c)  $\Pi$ -type, and (d) T-type, where C and L represent a capacitor and an inductor, respectively, and TL represents any circuit element that contains resistance, capacitance, or inductance, redrawn from [144] (pp. 229, 390).

#### 4.3. Rectification Circuits

The third component in wireless energy harvesting is the rectifier, which converts AC electricity into DC electricity. There are two classes of rectifiers: half-wave and full-wave rectifiers. The half-wave rectifier comprises of a single diode (Figure 12a), through which only the positive half of the AC input voltage is passed and the negative half is removed [12]. Consequently, the half-wave method leaves the discontinuity in the output voltage and has a low efficiency [12].

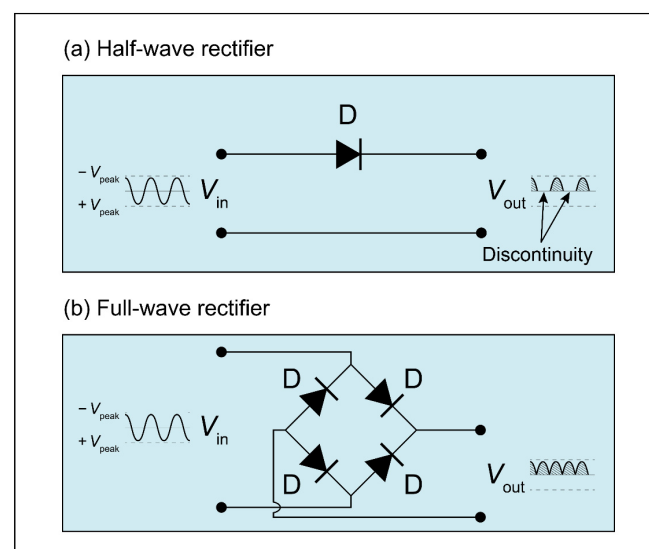


**Figure 12.** Schematic illustration of (a) half-wave and (b) full-wave (bridge) rectifiers, where  $D$ ,  $V_{in}$ , and  $V_{out}$  respectively represent a diode, the input voltage and the output voltage, redrawn from [12] (p. 9).

In order to improve both ripple factor and conversion efficiency, the full-wave rectifier was conceived. As depicted in Figure 12b, the full-wave rectifier may consist of four alternatively blocking pairs of diodes to rectify both positive and negative cycles [12]. Although structurally more complex, the full-wave configuration is more preferable for wireless energy harvesting applications, where available energy is limited, and a higher efficiency is of crucial factor.

A voltage multiplier is a special kind of rectifier circuit that converts AC electricity into higher-voltage DC electricity and is widely used in ambient wireless energy harvesting applications, where an enhancement of the output voltage is crucial [12,83]. Voltage multipliers can be generally divided into half-wave and full-wave multipliers and their common topologies are shown in Figure 13. In the half-wave voltage multiplier (Figure 13a), the first capacitor ( $C_1$ ) is charged during the negative cycle, whereas the second capacitor ( $C_2$ ) is charged during the following positive cycle; consequently, the output voltage is doubled as it sees two capacitors in series [12]. The similar mechanisms is due for the full-wave voltage multiplier (Figure 13b), however, because of a higher current driving capability, the full-wave architecture has an advantage of better stability in exchange for structural complexity [153].

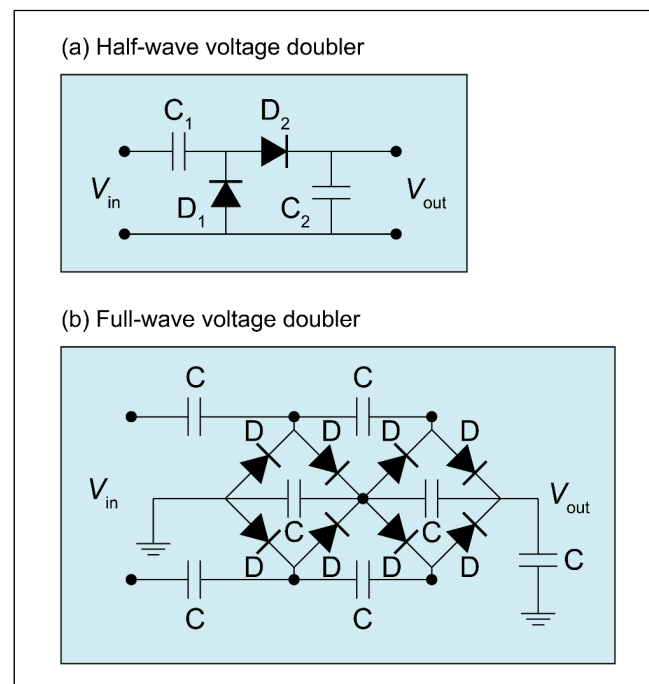


**Figure 13.** Schematic illustration of (a) half-wave and (b) full-wave (Cockcroft–Walton) voltage multipliers, redrawn from [154] (p. 29) and [153] (p. 389).

#### 4.4. Loads

The last component in wireless energy harvesting is the load, which can be an application device such as a wireless sensor node [142,155]. However, if a higher power is necessary, the harvested energy can be stored in a buffer such as a rechargeable battery or a supercapacitor until there is sufficient power to support the application device (Figure 5) [155]. Details on the wearable batteries and supercapacitors are available in [156–159].

### 5. Textile Materials for Wireless Energy Harvesting

#### 5.1. Electrically Insulating and Conductive Textile Materials

Textile materials offer unique advantages over the conventional, rigid materials such as PCBs, and those include the flexibility, tenacity, breathability, and aesthetic appearance that are exceedingly suitable for wearable applications [106,107,160–163]. In addition,

because clothing offers a considerable surface area, more than one textile rectenna could be integrated into clothing to uplift the harvestable energy.

As described in Section 4, a rectenna, an enabling element of wireless energy harvesting, consists of a receiving antenna, an impedance matching network, and a rectification circuit. In order to fabricate these components with textile materials, two types of materials are necessary: electrically insulating and conductive textiles.

Electrically insulating textile materials are ordinary (conventional) fibers, yarns, and fabrics that do not actively support a flow of electrons but provide an electrical insulation. Some examples of electrically insulating textiles are cotton, wool, silk, polyesters, polyamides, and polyurethanes, whose electrical conductivities are practically negligible [164]. Electrically insulating textiles have a consequential role of preventing electrical leakage between conductors but also serve as a dielectric medium to store (or dissipate) electrical energy under an applied electric field [165]. The latter function has found a variety of uses in microwave engineering including wireless energy harvesting, where the properties of dielectric materials (i.e., dielectric constant and loss tangent) largely determine the end-product performance [114,133,134].

One of the key features of using textile-based dielectrics in rectenna development is that they typically offer a relatively low dielectric constant and loss tangent because of their highly porous nature (Table 2) [107–109,165–169]. Since the antenna parameters such as gain, efficiency and bandwidth can be improved by lowering the dielectric constant and/or loss tangent, the use of textile materials could improve the overall energy harvesting efficiency [107,114,133,134,165,170,171].

**Table 2.** Dielectric properties of electrically insulating materials.

Material	Construction	Characterization Frequency (GHz)	Relative Humidity (%)	Dielectric Constant	Loss Tangent	References	
Textile (fabric)	Cotton	Plain weave	~2.45	80 ± 2.5	1.24–1.46	–	[170]
				65 ± 5	1.24–1.43		
				50 ± 2.5	1.26–1.38		
				35 ± 2.5	1.21–1.35		
				20 ± 2.5	1.18–1.31		
			1.1	65	1.875–2.499	0.0950–0.1355	[172]
		Twill weave	2.45		1.71	0.020	[173]
			1.1	65	1.858–1.940	0.1012–0.1053	[172]
		Satin weave	1.1	65	1.649	0.0859	[172]
		Single jersey	~2.45	80 ± 2.5	1.37–1.62	–	[170]
	65 ± 5			1.35–1.59			
	50 ± 2.5			1.30–1.50			
	35 ± 2.5			1.28–1.47			
	20 ± 2.5			1.23–1.40			
	Polyester	Plain weave	2.26	–	1.55	0.0087	[108]
Fleece		2.45	–	1.15	0.000	[173]	
3D spacer knit		2.25	–	1.10–1.13	0.004–0.018	[169]	

Table 2. Cont.

Material	Construction	Characterization Frequency (GHz)	Relative Humidity (%)	Dielectric Constant	Loss Tangent	References
Cordura®	–	2.45	–	1.93	0.015	[174]
Kevlar®	3D orthogonal weave	1.9	–	1.96	0.042	[175]
E-glass	3D orthogonal weave	1.5	–	3.2	0.008	[176]
Non-textile	Cellulose film	7.3	(Dry condition)	~3.2	~0.03	[177]
	Poly(ethylene terephthalate)	2.45	–	~2.1–2.4	~0.016–0.04 *	[178]
	Standard FR4	2.08–3.70	–	4.5	0.035	[179]
	Rogers RT/duroid® 5870	8–40 (dielectric constant) and 10 (loss tangent)	–	2.33	0.0012	[180]

\* Calculated by the formula  $\tan \delta = \epsilon_r'' / \epsilon_r'$ , where  $\tan \delta$  is the loss tangent,  $\epsilon_r''$  is the imaginary part of the relative permittivity and  $\epsilon_r'$  is the real part of the relative permittivity (dielectric constant).

Yet, the use of textile materials brings a latent concern for rectenna development. The dielectric properties of moisture-absorbing materials such as cotton are reported to be highly susceptible to the relative humidity of the environment (Table 2); consequently, rectennas made of hygroscopic textiles may experience a shift in the resonant frequency and a reduction in the conversion efficiency during operation. Therefore, although moisture absorbing materials may be preferable from the sensorial comfort point of view [106,162,181,182], the effect of the relative humidity must be well-assessed in the rectenna design stage.

Electrically conductive textile materials, on the other hand, are fibers, yarns, and fabrics with a significant electrical conductivity. Because a higher electrical conductivity leads to lower conductor-related losses [183,184], improvement in the electrical conductivity has been a primary research interest for textile materials over the past several decades.

Since the ordinary textile materials do not possess a tangible electrical conductivity, a special preparation is required to attain good conductivity. A variety of fabrication methods have been developed for electrically conductive fabrics, but the most fundamental approach is to produce electrically conductive fibers, which can then be transformed into yarns for integration into fabrics. There are four general routes to electrically conductive fibers and are depicted in Figure 14.

In the first route, electrically conductive metals such as silver and copper are converted into metal fibers by wire drawing [185]. The advantages of this method include the high electrical conductivity and a high-temperature stability of bulk metals (Table 3), in exchange for a high rigidity and fatigue-related concerns [186].



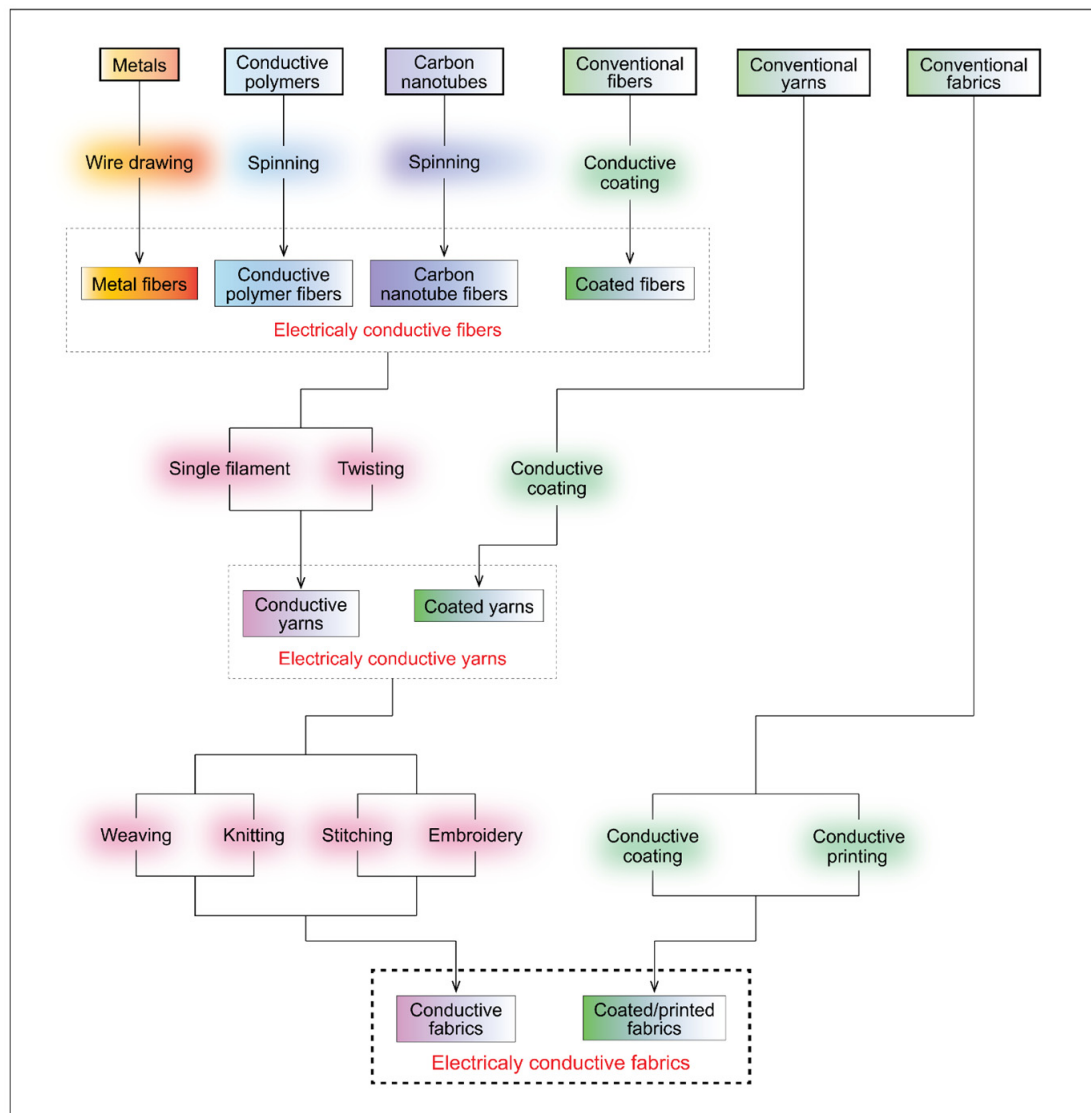


**Figure 14.** From raw materials to electrically conductive fabrics.

**Table 3.** DC electrical properties of electrically conductive materials.

	Material	Construction	Conductivity (S/m)	Sheet Resistance ( $\Omega$ /Square)	References
Textile (Fabric)	Copper/nickel-plated polyamide	Ripstop	$4.17 \times 10^6$	0.03	[183]
	Silver/copper/nickel-plated polyamide	Ripstop	–	0.009	[187]
	Silver-plated polyamide	Single jersey	$2.08 \times 10^{-1}$	–	[188]
	Carbon-nanotube-coated cotton	Knit	$1.25 \times 10^4$	<1	[189]
	PEDOT-coated polyester	Woven	–	52	[190]
	Silver-printed polyester	Nonwoven	–	<0.025	[191]
	Silver-printed Evolon®	Nonwoven	$1.3 \times 10^6$	–	[192]
	Lycra® with silver yarn	Woven	–	0.6	[193]

Table 3. Cont.

	Material	Construction	Conductivity (S/m)	Sheet Resistance ( $\Omega$ /Square)	References
Non-textile (Bulk material)	Silver	–	$6.3 \times 10^7$ *	–	[194]
	Copper	–	$6.0 \times 10^7$ *	–	[194]
	Gold	–	$4.4 \times 10^7$ *	–	[194]
	PEDOT	–	$1 \times 10^5$	–	[190]

\* Calculated by taking the reciprocal of electrical resistivity.

The second approach is based on conductive polymers, which exhibit a good electrical conductivity. Since the discovery of the first conductive polymer by Shirakawa et al. in 1977 [195], a variety of conductive polymers such as polyaniline, polythiophenes, PEDOT, PEDOT:PSS, and polypyrrole have been synthesized. The underlying mechanism responsible for electrical conduction by these polymers is a conjugated structure that enables the delocalization of  $\pi$  electrons across adjacent p orbitals and hence electrical conduction is achieved [196]. Fibers can be formed from conductive polymers by conventional spinning methods such as melt spinning, wet spinning, or electrospinning [197], and those fibers have excellent flexibility as a soft yarn [198] but typically with a limited electrical conductivity (Table 3) [199].

Being well-recognized for their exceptional conductivities and mechanical strengths, carbon nanotubes have also been transformed into fiber forms by various spinning techniques such as forest spinning, direct spinning, or solution spinning [200]. However, one of the current challenges with carbon nanotube fibers is the limited industrial scalability for high quality, continuous carbon nanotube fiber production due to the complex fabrication procedure [201].

The last category of electrically conductive fibers is coated fibers, which can be produced by coating the surface of a conventional, electrically insulating fiber with an electrically conductive substance. Two of the most widely used coating methods are electroplating and electroless plating usually with a high-conductivity metals such as silver, copper, or gold, and finished fibers have advantages of good electrical conductivity, flexibility, durability, and processability [202,203].

An electrically conductive yarn is a monofilament yarn or a bundle of fibers, where the latter can be produced by twisting electrically conductive fibers alone for an enhanced electrical conductance or with conventional fibers for a better processability (Figure 14) [204]. Additionally, electrically conductive yarns can also be produced by coating conventional yarns with electrically conductive materials such as metals [205].

Electrically conductive fabrics can be produced in two different ways. In the first way, electrically conductive yarns are converted into fabric forms by a conventional textile processing technique such as weaving [176,206], knitting [204], stitching [207,208], or embroidering [209–211]. While these processes have an advantage of seamless integration as the electrically conductive components are inherently embedded into a fabric, relatively strict requirements are imposed on the yarn mechanical properties. For instance, warp yarns for weaving need to have a higher tenacity to withstand a high tension during weaving, whereas yarns for knitting, stitching, and embroidery are required to be of lower bending modulus to be able to form small loops [212,213]. Therefore, while these processes could realize a sufficiently high conductivity (Table 3), yarns that do not have suitable mechanical properties may not be processed by these techniques.

The second method involves coating with an electrically conductive substance. Similar to the preparation of electrically conductive fibers and yarns, electrically conductive fabrics can also be produced by coating conventional fabrics with an electrically conductive material to attain good electrical properties (Table 3) [183,188–190]. In addition, a highly

conductive coating layer can also be formed by screen or inkjet printing with an electrically conductive ink (Table 3) [191,192,214–216].

### 5.2. Textile-Based Antennas

Textile antennas can be produced by a variety of techniques from electrically conductive and insulating fibers, yarns, and fabrics. For instance, a patch antenna, which is the most widely investigated antennas for wearable energy harvesting applications [128–130], can be fabricated in aesthetic and comfortable form factors simply by stacking conductive and dielectric fabrics [106,108,109,162] (Figure 15a) but also by a fundamental textile processing technique such as weaving [175,176,217,218], knitting [219], or embroidery [220–222] with conductive and insulating threads, or by printing electrically conductive inks on electrically insulating fabrics [192]. In a similar way, many of the other antenna structures such as dipole (Figure 15b) [211,223,224], bowtie (Figure 15c) [225], spiral (Figure 15d) [226], slot (Figure 15e) [187,227], Vivaldi [228], Yagi-Uda [193], log-periodic array [229], antennas can also be produced in textile forms by adapting these techniques.

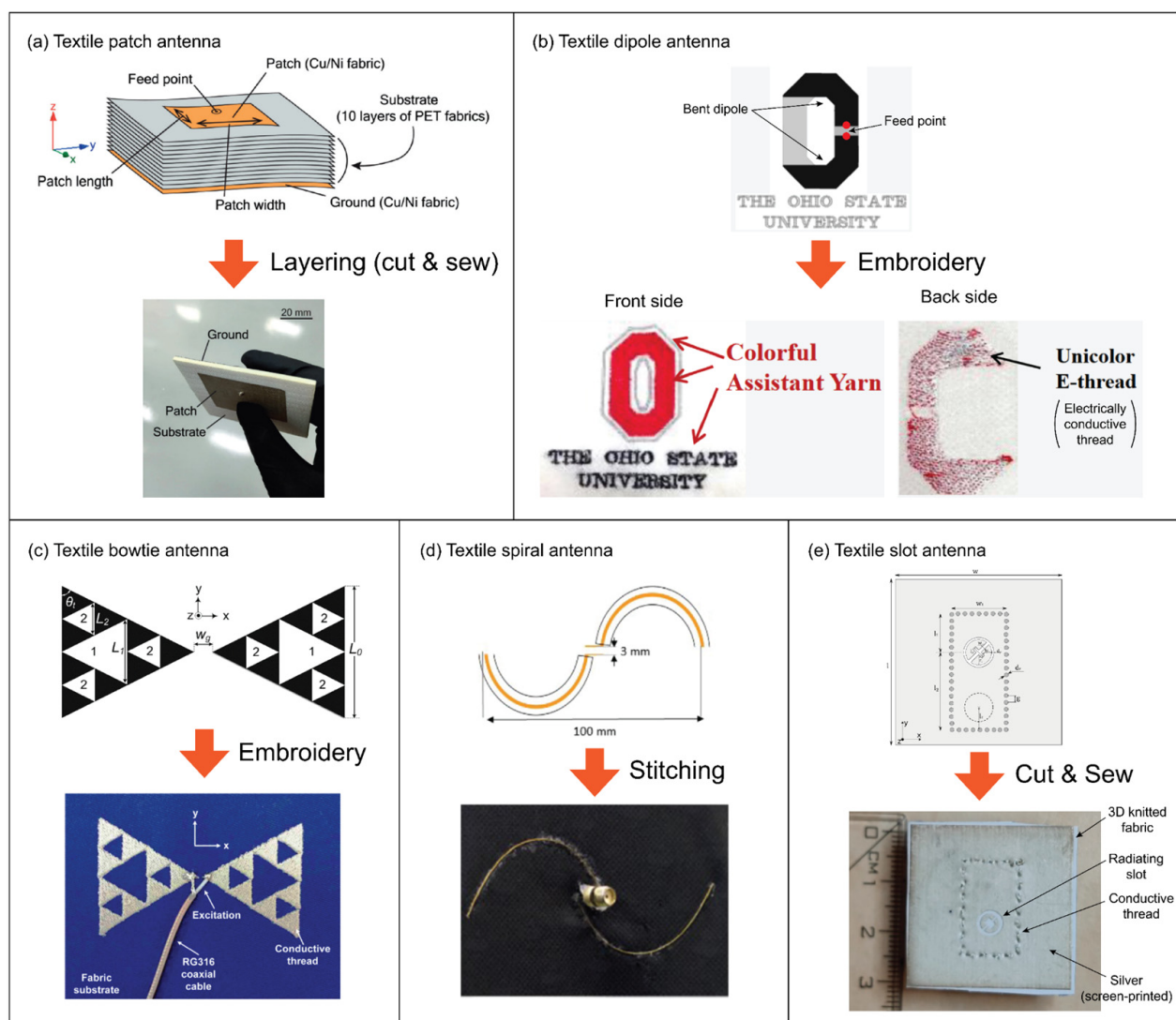


**Figure 15.** Textile antennas for wearable applications: (a) textile patch antenna made by stacking polyester and copper/nickel-plated polyester fabrics, adapted from [108] (pp. 2792, 2794) © 2019 Yusuke Mukai, Vivek T. Bharambe, Jacob J. Adams and Minyoung Suh, (b) textile dipole antenna

embroidered with an electrically conductive thread, adapted under a Creative Commons Attribution 4.0 License from [223] (p. 373) © 2015 Asimina Kiourti and John L. Volakis, (c) textile bowtie antenna embroidered with a silver-plated copper thread, adapted under a Creative Commons Attribution 4.0 License from [225] (pp. 3–4) © 2021 Theodoros N. Kapetanakis, Martin Pavec, Melina P. Ioannidou, Christos D. Nikolopoulos, Anargyros T. Baklezos, Radek Soukup and Ioannis O. Vardiambasis, (d) textile spiral antenna stitched with a silver/polyimide-coated silica fiber, adapted under a Creative Commons Attribution 4.0 License from [226] (p. 7) © 2018 Mourad Roudjane, Mazen Khalil, Amine Miled and Younés Messaddeq, and (e) 3D-knitted slot antenna screen-printed with a silver paste and sewn with a conductive thread, adapted under a Creative Commons Attribution 4.0 License from [227] (pp. 3, 9) © 2022 Miroslav Cupal and Zbynek Raida.

### 5.3. Textile-Based Impedance Matching Networks

As discussed in Section 4, a variety of impedance matching techniques have been developed in the literature, and in theory, any of them could be employed for rectennas. However, for textile rectennas, tuning stubs are probably the most widely employed matching networks since they involve a small number of components and soldering points; they are relatively simple to fabricate [24]. An example of a textile-based single tuning stub is given in Figure 16a. The open-circuit shunt stub made of a highly conductive copper-plated polyester fabric was placed between the microstrip feed line and rectification circuit to maximize the energy transfer from the receiving antenna to the rectifier.

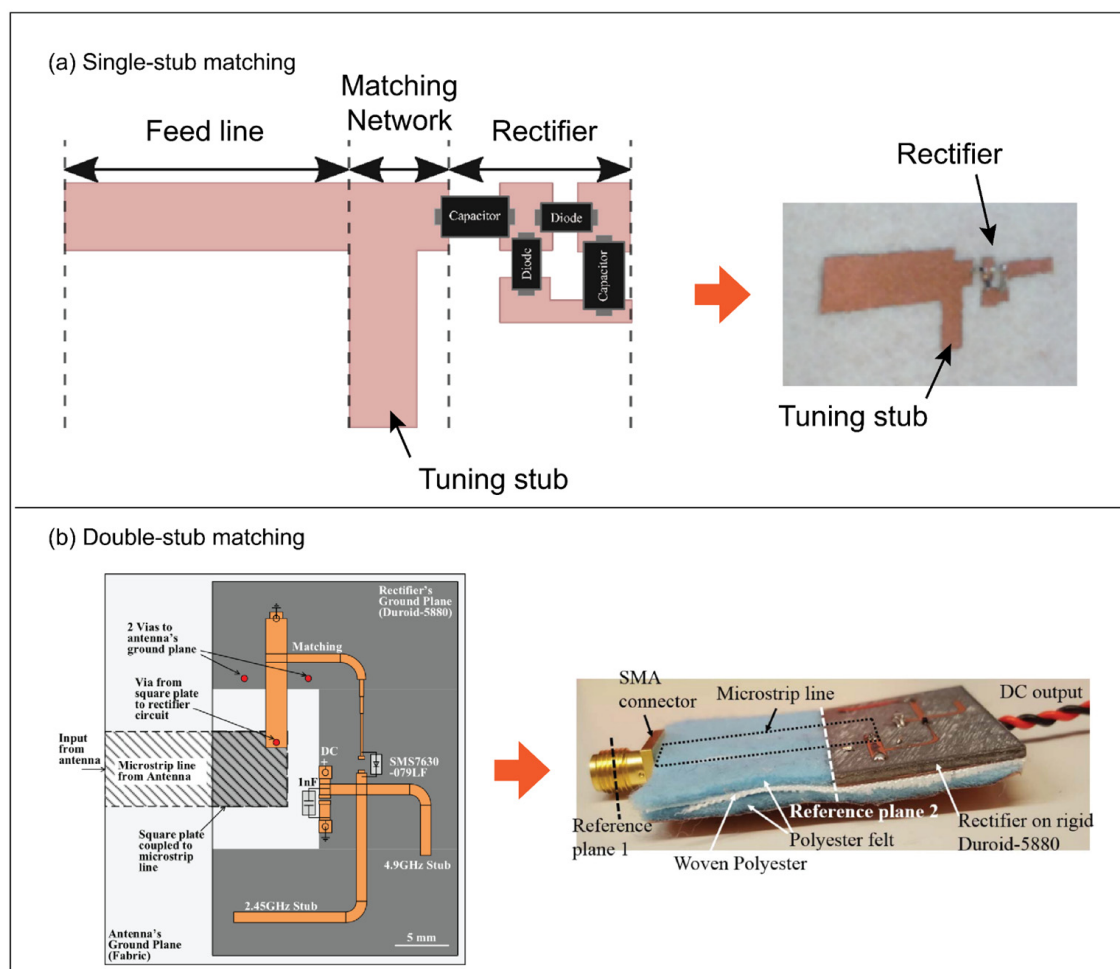


**Figure 16.** Textile-integrated matching networks: (a) open-circuit single stub made of a copper-plated polyester fabric and a felt, adapted under a Creative Commons Attribution 4.0 License from [24]

(pp. 7, 11) © 2021 by Juan-Manuel Lopez-Garde, Ruben Del-Rio-Ruiz, Jon Legarda and Hendrik Rogier, and (b) open-circuit double stubs made of a PCB (RT/Duroid® 5880) integrated with textile materials, adapted under a Creative Commons Attribution 3.0 License from [68] (p. 385) © 2018 by Salah-Eddine Adami, Plamen Proynov, Geoffrey S. Hilton, Guang Yang, Chunhong Zhang, Dibin Zhu, Yi Li, Steve P. Beeby, Ian J. Craddock and Bernard H. Stark.

A double stub tuning network, which was fabricated on a textile-integrated PCB, is shown in Figure 16b. Although the double-stub network requires fabrication of the second stub and is more space-demanding, this additional component was demonstrated to support the second harmonics; consequently, the output power was calculated to be improved by about 1% (compared with a single-stub counterpart) [68]. However, because of the rigidity of the PCB-based impedance matching network, the flexibility and conformity of this structure was impaired.

#### 5.4. Textile-Based Rectification Circuits

Among the various rectification circuit options available, the full-wave (bridge) rectifier (Figure 12b) and voltage doubler (Figure 13a) are commonly used in textile-based wireless energy harvesters as they are a good compromise between the circuit complexity and rectification efficiency [24]. In realizing a rectification circuit on a textile platform, diodes and capacitors can be soldered to electrically conductive textile materials. For instance, Lopez-Garde et al. soldered commercially available Schottky diodes and capacitors to an electrically conductive copper fabric to create a voltage doubler (Figure 17) [24]. The dimensions of the textile voltage doubler were optimized by using a computer-aided software (Keysight Advanced Design System) to achieve a rectification efficiency of 56%.

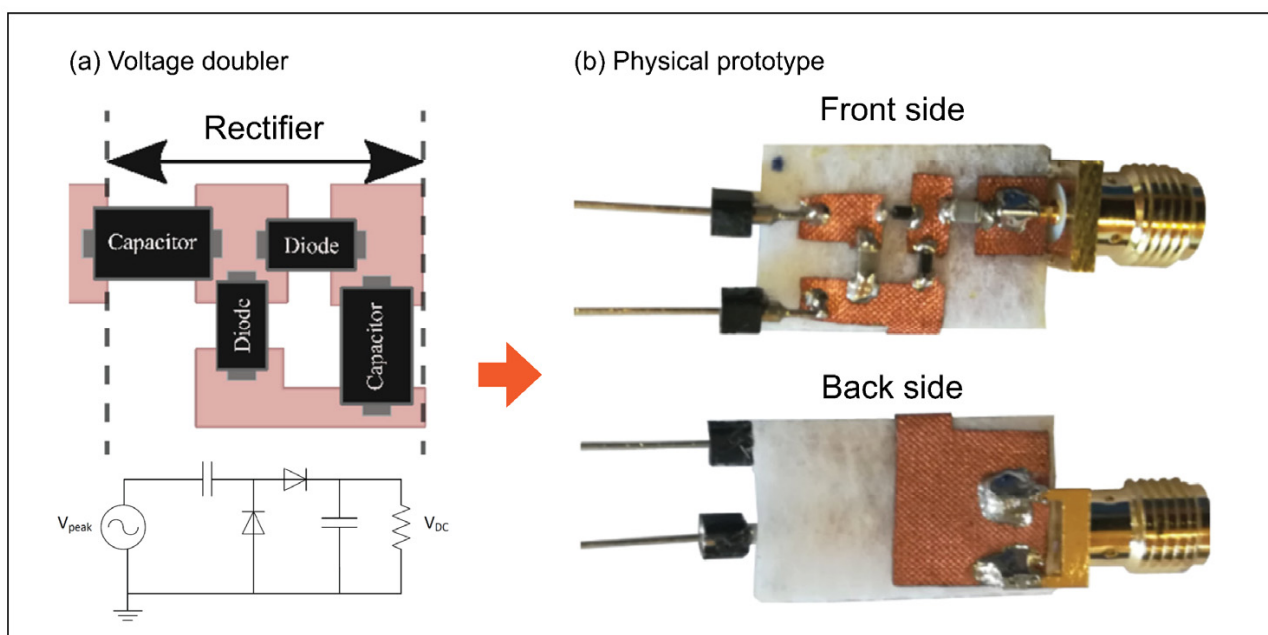


**Figure 17.** Schematic illustration of (a) a voltage doubler and (b) its physical prototype built of the same textile materials shown in Figure 16a and commercially available diodes and capacitors, adapted under a Creative Commons Attribution 4.0 License from [24] (pp. 6–7) © 2021 by Juan-Manuel Lopez-Garde, Ruben Del-Rio-Ruiz, Jon Legarda and Hendrik Rogier.

Another textile-based rectification circuit was presented by Vital et al. and was fabricated by soldering a Schottky diode to an organza fabric embroidered with an electrically conductive thread (silver-plated copper strands) [84]. The diode was connected to a transmission line on each end, but one of the transmission lines was shorted to generate a standing wave. In this configuration, by optimizing the lengths of these two transmis-



sion lines, the power stored in the standing wave was successfully transformed into DC electricity with a rectification efficiency of 70% (at 8 dBm), which was far greater than the theoretical limit of half-wave rectifiers. Therefore, this strategy of extracting the negative half of the AC input electricity with a single diode not only improves the rectification efficiency of half-wave rectifiers but also enables a more minimalistic and hence mechanically flexible architecture particularly invaluable for wearable applications.

## 6. Current Research Mainstream and Future Perspectives

As reviewed so far, the use of textile materials in wearable wireless energy harvesting applications offers a variety of unique and often irreplaceable features, such as lightweight, flexible, breathable, low-profile, comfortable, and aesthetic form factors, and textile-based wireless energy harvesters can be inherently integrated into clothing with minimum alteration of its performance as an apparel product. In addition, several harvesting units can be incorporated into clothing, which offers a large surface area for such integration. This aspect is of particular interest for wireless energy harvesting applications, where the available ambient energy is limited and the amount of harvestable energy from a single rectenna element could be insufficient. For instance, Lopez-Garde et al. developed a 4-element ( $2 \times 2$  array) rectenna made of a copper-plated polyester fabric and a felt (Figure 18). It was reported that this 4-element rectenna was able to harvest 1.1 mW of DC power from an input power of  $14 \mu\text{W}/\text{cm}^2$ , while only 0.26 mW of DC power was harvested with a single-element rectenna [24].

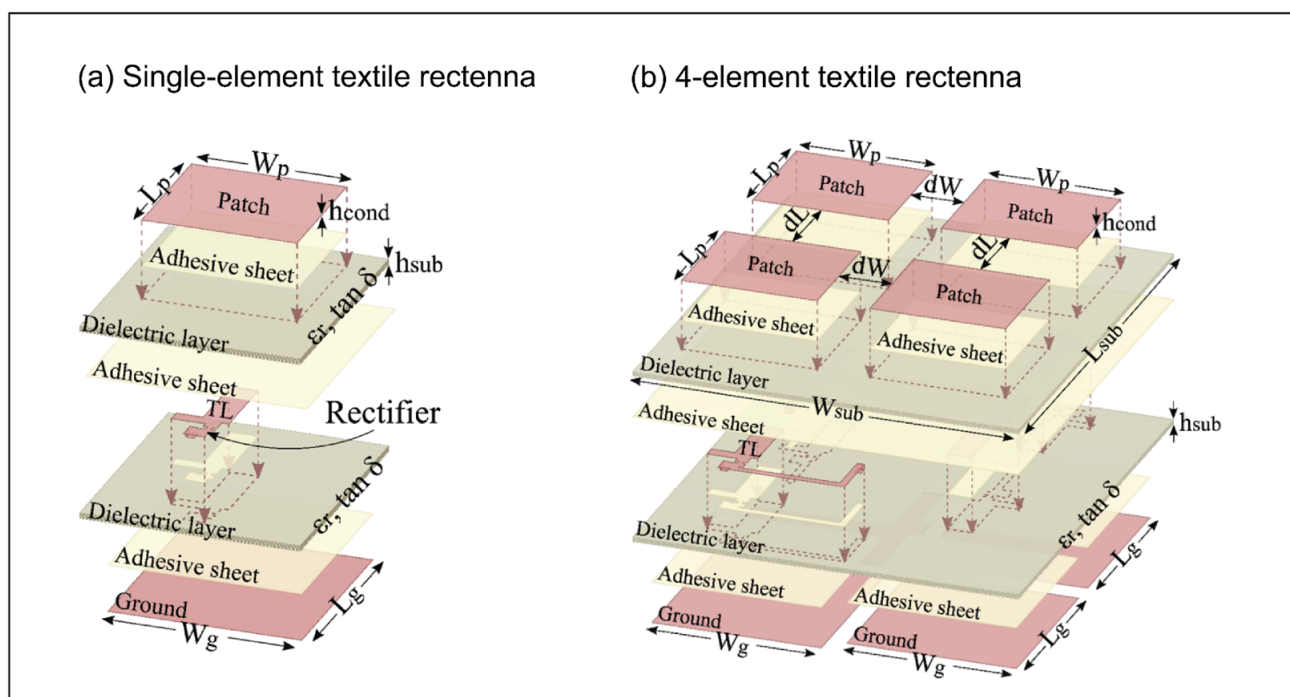


**Figure 18.** Schematic illustration of (a) single-element and (b) 4-element textile rectennas made of a copper-plated polyester fabric and a felt, reproduced under a Creative Commons Attribution 4.0 License from [24] (pp. 8, 10) © 2021 by Juan-Manuel Lopez-Garde, Ruben Del-Rio-Ruiz, Jon Legarda and Hendrik Rogier.

The use of multi-element rectenna was also reported by Vital et al., who developed  $2 \times 2$  and  $2 \times 3$  rectenna arrays made of an organza fabric embroidered with an electrically conductive thread (Figure 19) [84]. Under a natural ambient environment, it was demonstrated that the  $2 \times 2$  rectenna array can harvest up to  $100 \mu\text{W}$ , which was significantly higher than that of a single-element rectenna made of the same materials. In addition, the  $2 \times 3$  rectenna array was tested with Wi-Fi signals boosted by an external amplifier

and was able to generate a DC output power of up to 600  $\mu\text{W}$ . These results indicate that textile-based rectenna arrays could be a promising solution to power wearable electronics under a natural ambient environment, and if a higher power output is required, ambient signals could be amplified by an external device.

While textile-based rectenna arrays are propitious, there are also challenges. For instance, Estrada et al. developed T-shirt-integrated 16-element and 81-element rectenna arrays. The receiving antennas were bow-tie arrays that were produced by screen-printing an electrically conductive silver ink on a cotton fabric [230]. Although, a higher DC output is generally expected from a larger array, the measured output powers of these textile rectenna arrays were nevertheless not significantly different. The authors elucidated this observation that the resistivity of the screen-printed ink was relatively high and as such the efficiency have dropped as the array was scaled up in size. Therefore, an improvement of the electrical conductivity of textile materials is crucial for further advancement of multi-element arrays made of textile materials.

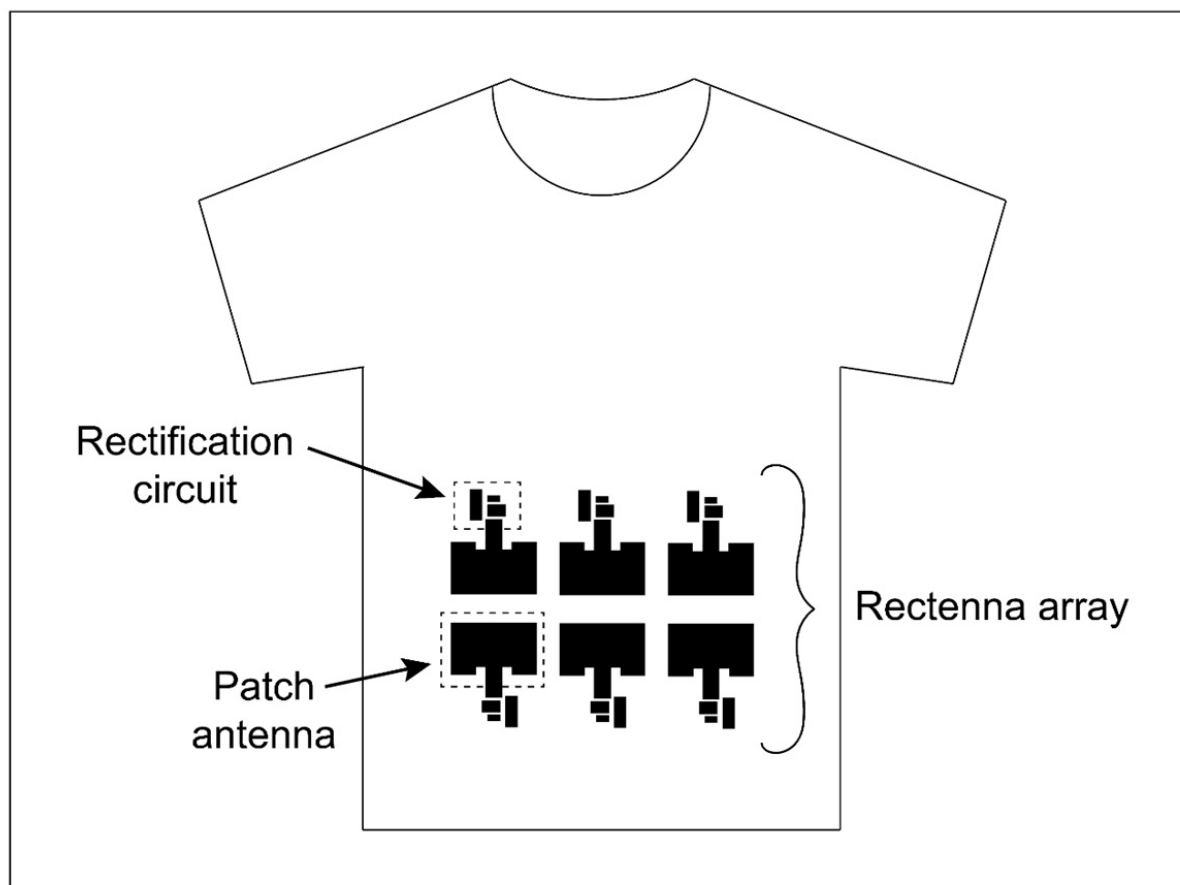


**Figure 19.** Six-element rectenna array integrated into clothing for wearable wireless power harvesting applications, redrawn from [84] (p. 1).

In addition, rectification circuits of textile rectennas found in the literature are predominantly constructed with commercially available rigid diodes, and as such the flexibility and conformity of current textile rectennas are impaired by these components. In addition, it has been pointed out that the rectification efficiency is largely capped by the relatively high cut-in voltage of commercial diodes under low ambient power conditions [231]. In order to overcome these limitations, an investigation on flexible (and preferably textile-based) diodes that enable a highly efficient rectification is pivotal in future work.

Another vital research topic is on the improvement of aesthetic appearance of textile-based wireless energy harvesters. As an apparel product, it is essential to have an aestheti-

cally pleasing design but this facet was often overlooked in early development of wearable electronics [232]. Currently, a variety of approaches have been proposed to accommodate both functionality and aesthetic look. For instance, Kiourti and Volakis developed a logo antenna made of textile materials [223]. As shown in Figure 15b, the slightly bent dipole antenna was seamlessly integrated into a fabric by embroidering an electrically conductive thread, and this was followed by another embroidery process with ordinary color threads to ensure that the antenna form part of logo and invisible from outside. The finished antenna was flexible, lightweight, and mechanically robust to withstand daily wear and repetitive washing and drying cycles [223], evidencing that functional and fashionable requirements could be met without a compromise. Further journey to improve the aesthetic performance and meet the essential criteria as apparel products would make the textile-based solutions to strongly appeal to healthcare, military, entertainment, and other relevant sectors.

## 7. Conclusions

This paper reviewed unmissable recent progress in textile-based wireless energy harvesters for powering body-worn electronics. Textiles are flexible, lightweight, breathable materials and could be ideal for the fabrication of wireless energy harvesting devices with excellent comfort and aesthetic appearance. Moreover, because clothing offers a substantial surface area, multiple harvesting units can be seamlessly integrated into clothes to enhance the output power.

For further advancement of the textile-based wireless energy harvesting technology, several future research topics were suggested. First, it is essential to improve the electrical conductivity of textile materials to reduce the conductor-related losses and increase the overall conversion efficiency. In addition, development of flexible (and ideally textile-based) diodes with a high rectification efficiency is vital to improve both conversion efficiency and wearability. Lastly, product design and aesthetics research is crucial for a broader acceptance of this emerging technology in various key sectors.

**Funding:** This research received no external funding.

**Conflicts of Interest:** The author declares no conflict of interest.

## References

1. Yamada, Y. Textile-Integrated Polymer Optical Fibers for Healthcare and Medical Applications. *Biomed. Phys. Eng. Express* **2020**, *6*, 062001. [CrossRef]
2. Yamada, Y.; Suh, M. Textile Materials for Mobile Health: Opportunities and Challenges. In Proceedings of the Presented at the WTiN Innovate Textile & Apparel Virtual Trade Show, Online, 15–30 October 2020.
3. Quandt, B.M.; Boesel, L.F.; Rossi, R.M. Polymer Optical Fibres in Healthcare: Solutions, Applications and Implications. A Perspective. *Polym. Int.* **2018**, *67*, 1150–1154. [CrossRef]
4. Winterhalter, C.A.; Teverovsky, J.; Wilson, P.; Slade, J.; Horowitz, W.; Tierney, E.; Sharma, V. Development of Electronic Textiles to Support Networks, Communications, and Medical Applications in Future U.S. Military Protective Clothing Systems. *IEEE Trans. Inf. Technol. Biomed.* **2005**, *9*, 402–406. [CrossRef]
5. Haagensohn, T.; Noghanian, S.; Leon, P.d.; Chang, Y. Textile Antennas for Spacesuit Applications: Design, Simulation, Manufacturing, and Testing of Textile Patch Antennas for Spacesuit Applications. *IEEE Antennas Propag. Mag.* **2015**, *57*, 64–73. [CrossRef]
6. Hartman, K.; Westecott, E.; Colpitts-Campbell, I.; Faber, J.R.; Shao, Y.; Luginbuhl, C.; Prior, O.; Laroia, M. Textile Game Controllers: Exploring Affordances of E-Textile Techniques as Applied to Alternative Game Controllers. In Proceedings of the Fifteenth International Conference on Tangible, Embedded, and Embodied Interaction, Salzburg, Austria, 14–17 February 2021; Association for Computing Machinery: New York, NY, USA, 2021; pp. 1–14.
7. Yin, L.; Kim, K.N.; Lv, J.; Tehrani, F.; Lin, M.; Lin, Z.; Moon, J.-M.; Ma, J.; Yu, J.; Xu, S.; et al. A Self-Sustainable Wearable Multi-Modular E-Textile Bioenergy Microgrid System. *Nat. Commun.* **2021**, *12*, 1542. [CrossRef]
8. Dolez, P.I. Energy Harvesting Materials and Structures for Smart Textile Applications: Recent Progress and Path Forward. *Sensors* **2021**, *21*, 6297. [CrossRef] [PubMed]
9. Hambling, D. The Overloaded Soldier: Why U.S. Infantry Now Carry More Weight Than Ever. Available online: <https://www.popularmechanics.com/military/research/a25644619/soldier-weight/> (accessed on 9 July 2022).

10. Zhang, Y.; Bai, W.; Cheng, X.; Ren, J.; Weng, W.; Chen, P.; Fang, X.; Zhang, Z.; Peng, H. Flexible and Stretchable Lithium-Ion Batteries and Supercapacitors Based on Electrically Conducting Carbon Nanotube Fiber Springs. *Angew. Chem. Int. Ed.* **2014**, *53*, 14564–14568. [[CrossRef](#)] [[PubMed](#)]
11. Kamalinejad, P.; Mahapatra, C.; Sheng, Z.; Mirabbasi, S.; Leung, V.C.M.; Guan, Y.L. Wireless Energy Harvesting for the Internet of Things. *IEEE Commun. Mag.* **2015**, *53*, 102–108. [[CrossRef](#)]
12. Tran, L.-G.; Cha, H.-K.; Park, W.-T. RF Power Harvesting: A Review on Designing Methodologies and Applications. *Micro Nano Syst. Lett.* **2017**, *5*, 14. [[CrossRef](#)]
13. Shafique, K.; Khawaja, B.A.; Khurram, M.D.; Sibtain, S.M.; Siddiqui, Y.; Mustaqim, M.; Chattha, H.T.; Yang, X. Energy Harvesting Using a Low-Cost Rectenna for Internet of Things (IoT) Applications. *IEEE Access* **2018**, *6*, 30932–30941. [[CrossRef](#)]
14. Hande, A.; Polk, T.; Walker, W.; Bhatia, D. Indoor Solar Energy Harvesting for Sensor Network Router Nodes. *Microprocess. Microsyst.* **2007**, *31*, 420–432. [[CrossRef](#)]
15. Tran, T.V.; Chung, W.-Y. High-Efficient Energy Harvester with Flexible Solar Panel for a Wearable Sensor Device. *IEEE Sens. J.* **2016**, *16*, 9021–9028. [[CrossRef](#)]
16. Zhang, S.; Bick, M.; Xiao, X.; Chen, G.; Nashalian, A.; Chen, J. Leveraging Triboelectric Nanogenerators for Bioengineering. *Matter* **2021**, *4*, 845–887. [[CrossRef](#)]
17. Perez, M.; Boisseau, S.; Gasnier, P.; Willemin, J.; Geisler, M.; Reboud, J.L. A Cm Scale Electret-Based Electrostatic Wind Turbine for Low-Speed Energy Harvesting Applications. *Smart Mater. Struct.* **2016**, *25*, 045015. [[CrossRef](#)]
18. Beeby, S.P.; Torah, R.N.; Tudor, M.J.; Glynne-Jones, P.; O'Donnell, T.; Saha, C.R.; Roy, S. A Micro Electromagnetic Generator for Vibration Energy Harvesting. *J. Micromech. Microeng.* **2007**, *17*, 1257–1265. [[CrossRef](#)]
19. Potnuru, A.; Tadesse, Y. Characterization of Pyroelectric Materials for Energy Harvesting from Human Body. *Integr. Ferroelectr.* **2014**, *150*, 23–50. [[CrossRef](#)]
20. Leonov, V.; Vullers, R.J.M. Wearable Thermoelectric Generators for Body-Powered Devices. *J. Electron. Mater.* **2009**, *38*, 1491–1498. [[CrossRef](#)]
21. Lee, F.Y.; Navid, A.; Pilon, L. Pyroelectric Waste Heat Energy Harvesting Using Heat Conduction. *Appl. Therm. Eng.* **2012**, *37*, 30–37. [[CrossRef](#)]
22. Qin, Y.; Wang, X.; Wang, Z.L. Microfibre–Nanowire Hybrid Structure for Energy Scavenging. *Nature* **2008**, *451*, 809–813. [[CrossRef](#)]
23. Wagih, M.; Hilton, G.S.; Weddell, A.S.; Beeby, S. Broadband Millimeter-Wave Textile-Based Flexible Rectenna for Wearable Energy Harvesting. *IEEE Trans. Microw. Theory Tech.* **2020**, *68*, 4960–4972. [[CrossRef](#)]
24. Lopez-Garde, J.-M.; Del-Rio-Ruiz, R.; Legarda, J.; Rogier, H. 2 × 2 Textile Rectenna Array with Electromagnetically Coupled Microstrip Patch Antennas in the 2.4 GHz WiFi Band. *Electronics* **2021**, *10*, 1447. [[CrossRef](#)]
25. Al-Husseini, M.; Haskou, A.; Rishani, N.; Kabalan, K.Y. Textile-Based Rectennas. In *Innovation in Wearable and Flexible Antennas*; Khaleel, H., Ed.; WIT Press: Southampton, UK, 2015; Volume 1, pp. 187–215, ISBN 978-1-84564-987-6.
26. Goncalves, R.; Carvalho, N.B.; Pinho, P.; Loss, C.; Salvado, R. Textile Antenna for Electromagnetic Energy Harvesting for GSM900 and DCS1800 Bands. In Proceedings of the 2013 IEEE Antennas and Propagation Society International Symposium (APSURSI), Orlando, FL, USA, 7–13 July 2013; pp. 1206–1207.
27. Tsolis, A.; Whittow, W.G.; Alexandridis, A.A.; Vardaxoglou, J.C. Embroidery and Related Manufacturing Techniques for Wearable Antennas: Challenges and Opportunities. *Electronics* **2014**, *3*, 314–338. [[CrossRef](#)]
28. Honan, G.; Gekakis, N.; Hassanali, M.; Nadeau, A.; Sharma, G.; Soyata, T. Energy Harvesting and Buffering for Cyber-Physical Systems: A Review. In *Cyber-Physical Systems: A Computational Perspective*; Siddesh, G.M., Deka, G.C., Srinivasa, K.G., Patnaik, L.M., Eds.; CRC Press: Boca Raton, FL, USA, 2015; pp. 210–237, ISBN 978-0-429-07616-9.
29. Zhang, N.; Chen, J.; Huang, Y.; Guo, W.; Yang, J.; Du, J.; Fan, X.; Tao, C. A Wearable All-Solid Photovoltaic Textile. *Adv. Mater.* **2016**, *28*, 263–269. [[CrossRef](#)] [[PubMed](#)]
30. Wu, C.; Kim, T.W.; Guo, T.; Li, F. Wearable Ultra-Lightweight Solar Textiles Based on Transparent Electronic Fabrics. *Nano Energy* **2017**, *32*, 367–373. [[CrossRef](#)]
31. Ku, M.-L.; Li, W.; Chen, Y.; Liu, K.J.R. Advances in Energy Harvesting Communications: Past, Present, and Future Challenges. *IEEE Commun. Surv. Tutor.* **2016**, *18*, 1384–1412. [[CrossRef](#)]
32. Satharasinghe, A.; Hughes-Riley, T.; Dias, T. Wearable and Washable Photovoltaic Fabrics. In Proceedings of the 36th European Photovoltaic Solar Energy Conference and Exhibition, Marseille, France, 9–13 September 2019; pp. 42–45.
33. Sugino, K.; Ikeda, Y.; Yonezawa, S.; Gennaka, S.; Kimura, M.; Fukawa, T.; Inagaki, S.; Konosu, Y.; Tanioka, A.; Matsumoto, H. Development of Fiber and Textile-Shaped Organic Solar Cells for Smart Textiles. *J. Fiber Sci. Technol.* **2017**, *73*, 336–342. [[CrossRef](#)]
34. Satharasinghe, A.; Hughes-Riley, T.; Dias, T. An Investigation of a Wash-durable Solar Energy Harvesting Textile. *Prog. Photovolt. Res. Appl.* **2020**, *28*, 578–592. [[CrossRef](#)]
35. Mokhtari, F.; Spinks, G.M.; Fay, C.; Cheng, Z.; Raad, R.; Xi, J.; Foroughi, J. Wearable Electronic Textiles from Nanostructured Piezoelectric Fibers. *Adv. Mater. Technol.* **2020**, *5*, 1900900. [[CrossRef](#)]
36. Lee, M.; Chen, C.-Y.; Wang, S.; Cha, S.N.; Park, Y.J.; Kim, J.M.; Chou, L.-J.; Wang, Z.L. A Hybrid Piezoelectric Structure for Wearable Nanogenerators. *Adv. Mater.* **2012**, *24*, 1759–1764. [[CrossRef](#)]
37. Li, S.; Zhong, Q.; Zhong, J.; Cheng, X.; Wang, B.; Hu, B.; Zhou, J. Cloth-Based Power Shirt for Wearable Energy Harvesting and Clothes Ornamentation. *ACS Appl. Mater. Interfaces* **2015**, *7*, 14912–14916. [[CrossRef](#)]



38. Somkuwar, V.U.; Pragya, A.; Kumar, B. Structurally Engineered Textile-Based Triboelectric Nanogenerator for Energy Harvesting Application. *J. Mater. Sci.* **2020**, *55*, 5177–5189. [[CrossRef](#)]
39. Li, X.; Sun, Y. WearETE: A Scalable Wearable E-Textile Triboelectric Energy Harvesting System for Human Motion Scavenging. *Sensors* **2017**, *17*, 2649. [[CrossRef](#)] [[PubMed](#)]
40. Zheng, Y.; Zhang, Q.; Jin, W.; Jing, Y.; Chen, X.; Han, X.; Bao, Q.; Liu, Y.; Wang, X.; Wang, S.; et al. Carbon Nanotube Yarn Based Thermoelectric Textiles for Harvesting Thermal Energy and Powering Electronics. *J. Mater. Chem. A* **2020**, *8*, 2984–2994. [[CrossRef](#)]
41. Sun, T.; Zhou, B.; Zheng, Q.; Wang, L.; Jiang, W.; Snyder, G.J. Stretchable Fabric Generates Electric Power from Woven Thermoelectric Fibers. *Nat. Commun.* **2020**, *11*, 572. [[CrossRef](#)]
42. Mitcheson, P.D.; Yeatman, E.M. Energy Harvesting for Pervasive Computing. *PerAda Mag.* **2008**, 1–3. [[CrossRef](#)]
43. Pillai, V.; Heinrich, H.; Dieska, D.; Nikitin, P.V.; Martinez, R.; Rao, K.V.S. An Ultra-Low-Power Long Range Battery/Passive RFID Tag for UHF and Microwave Bands with a Current Consumption of 700 nA at 1.5 V. *IEEE Trans. Circuits Syst. Regul. Pap.* **2007**, *54*, 1500–1512. [[CrossRef](#)]
44. Chen, W.; Che, W.; Yan, N.; Tan, X.; Min, H. Ultra-Low Power Truly Random Number Generator for RFID Tag. *Wirel. Pers. Commun.* **2011**, *59*, 85–94. [[CrossRef](#)]
45. Chang, Y.F.; Chen, C.S.; Zhou, H. Smart Phone for Mobile Commerce. *Comput. Stand. Interfaces* **2009**, *31*, 740–747. [[CrossRef](#)]
46. Danbatta, S.J.; Varol, A. Comparison of Zigbee, Z-Wave, Wi-Fi, and Bluetooth Wireless Technologies Used in Home Automation. In Proceedings of the 2019 7th International Symposium on Digital Forensics and Security (ISDFS), Barcelos, Portugal, 10–12 June 2019; pp. 1–5.
47. Kim, S.; Cho, N.; Song, S.; Kim, D.; Kim, K.; Yoo, H. A Sub 1V 96 mW Fully Operational Digital Hearing Aid Chip with Internal Status Controller. In Proceedings of the 32nd European Solid-State Circuits Conference, Montreaux, Switzerland, 19–21 September 2006; pp. 231–234.
48. Jiang, F. Investigation of Solar Energy for Photovoltaic Application in Singapore. In Proceedings of the 2007 International Power Engineering Conference (IPEC 2007), Singapore, 3–6 December 2007; pp. 86–89.
49. Duan, Y.; Zhao, G.; Liu, X.; Ma, J.; Chen, S.; Song, Y.; Pi, X.; Yu, X.; Yang, D.; Zhang, Y.; et al. Low-Temperature Processed Tantalum/Niobium Co-Doped TiO<sub>2</sub> Electron Transport Layer for High-Performance Planar Perovskite Solar Cells. *Nanotechnology* **2021**, *32*, 245201. [[CrossRef](#)]
50. Huang, J.; Zhou, Y.; Ning, Z.; Gharavi, H. Wireless Power Transfer and Energy Harvesting: Current Status and Future Prospects. *IEEE Wirel. Commun.* **2019**, *26*, 163–169. [[CrossRef](#)] [[PubMed](#)]
51. Montero, K.L.; Laurila, M.-M.; Mäntysalo, M. Effect of Electrode Structure on the Performance of Fully Printed Piezoelectric Energy Harvesters. *IEEE J. Flex. Electron.* **2022**, *1*, 24–31. [[CrossRef](#)]
52. Niu, X.; Jia, W.; Qian, S.; Zhu, J.; Zhang, J.; Hou, X.; Mu, J.; Geng, W.; Cho, J.; He, J.; et al. High-Performance PZT-Based Stretchable Piezoelectric Nanogenerator. *ACS Sustain. Chem. Eng.* **2019**, *7*, 979–985. [[CrossRef](#)]
53. Chang, C.; Tran, V.H.; Wang, J.; Fuh, Y.-K.; Lin, L. Direct-Write Piezoelectric Polymeric Nanogenerator with High Energy Conversion Efficiency. *Nano Lett.* **2010**, *10*, 726–731. [[CrossRef](#)]
54. González, J.L.; Rubio, A.; Moll, F. Human Powered Piezoelectric Batteries to Supply Power to Wearable Electronic Devices. *Int. J. Soc. Mater. Eng. Resour.* **2002**, *10*, 34–40. [[CrossRef](#)]
55. Zhang, X.-S.; Brugger, J.; Kim, B. A Silk-Fibroin-Based Transparent Triboelectric Generator Suitable for Autonomous Sensor Network. *Nano Energy* **2016**, *20*, 37–47. [[CrossRef](#)]
56. Zhu, G.; Zhou, Y.S.; Bai, P.; Meng, X.S.; Jing, Q.; Chen, J.; Wang, Z.L. A Shape-Adaptive Thin-Film-Based Approach for 50% High-Efficiency Energy Generation Through Micro-Grating Sliding Electrification. *Adv. Mater.* **2014**, *26*, 3788–3796. [[CrossRef](#)]
57. Lin, Z.; Chen, J.; Li, X.; Zhou, Z.; Meng, K.; Wei, W.; Yang, J.; Wang, Z.L. Triboelectric Nanogenerator Enabled Body Sensor Network for Self-Powered Human Heart-Rate Monitoring. *ACS Nano* **2017**, *11*, 8830–8837. [[CrossRef](#)] [[PubMed](#)]
58. Song, Y.; Wang, H.; Cheng, X.; Li, G.; Chen, X.; Chen, H.; Miao, L.; Zhang, X.; Zhang, H. High-Efficiency Self-Charging Smart Bracelet for Portable Electronics. *Nano Energy* **2019**, *55*, 29–36. [[CrossRef](#)]
59. Leonov, V. Human Machine and Thermoelectric Energy Scavenging for Wearable Devices. *ISRN Renew. Energy* **2011**, *2011*, 1–11. [[CrossRef](#)]
60. Nozariasbmarz, A.; Kishore, R.A.; Poudel, B.; Saparamadu, U.; Li, W.; Cruz, R.; Priya, S. High Power Density Body Heat Energy Harvesting. *ACS Appl. Mater. Interfaces* **2019**, *11*, 40107–40113. [[CrossRef](#)] [[PubMed](#)]
61. Lv, J.-R.; Ma, J.-L.; Dai, L.; Yin, T.; He, Z.-Z. A High-Performance Wearable Thermoelectric Generator with Comprehensive Optimization of Thermal Resistance and Voltage Boosting Conversion. *Appl. Energy* **2022**, *312*, 118696. [[CrossRef](#)]
62. Enescu, D. Thermoelectric Energy Harvesting: Basic Principles and Applications. In *Green Energy Advances*; Enescu, D., Ed.; IntechOpen: London, UK, 2019; ISBN 978-1-78984-199-2.
63. Thielen, M.; Sigrist, L.; Magno, M.; Hierold, C.; Benini, L. Human Body Heat for Powering Wearable Devices: From Thermal Energy to Application. *Energy Convers. Manag.* **2017**, *131*, 44–54. [[CrossRef](#)]
64. Guo, L.; Gu, X.; Chu, P.; Hemour, S.; Wu, K. Collaboratively Harvesting Ambient Radiofrequency and Thermal Energy. *IEEE Trans. Ind. Electron.* **2020**, *67*, 3736–3746. [[CrossRef](#)]

65. Pinuela, M.; Mitcheson, P.D.; Lucyszyn, S. Ambient RF Energy Harvesting in Urban and Semi-Urban Environments. *IEEE Trans. Microw. Theory Tech.* **2013**, *61*, 2715–2726. [\[CrossRef\]](#)
66. Sherazi, H.H.R.; Zorbas, D.; O'Flynn, B. A Comprehensive Survey on RF Energy Harvesting: Applications and Performance Determinants. *Sensors* **2022**, *22*, 2990. [\[CrossRef\]](#)
67. Monti, G.; Corchia, L.; Tarricone, L. UHF Wearable Rectenna on Textile Materials. *IEEE Trans. Antennas Propag.* **2013**, *61*, 3869–3873. [\[CrossRef\]](#)
68. Adami, S.-E.; Proynov, P.; Hilton, G.S.; Yang, G.; Zhang, C.; Zhu, D.; Li, Y.; Beeby, S.P.; Craddock, I.J.; Stark, B.H. A Flexible 2.45-GHz Power Harvesting Wristband with Net System Output from  $-24.3$  dBm of RF Power. *IEEE Trans. Microw. Theory Tech.* **2018**, *66*, 380–395. [\[CrossRef\]](#)
69. Khalifa, S.; Lan, G.; Hassan, M.; Hu, W.; Seneviratne, A. Human Context Detection from Kinetic Energy Harvesting Wearables. In *Examining Developments and Applications of Wearable Devices in Modern Society*; Silva, S.E.D., Oliveira, R.A.R., Loureiro, A.A.F., Eds.; IGI Global: Hershey, PA, USA, 2018; pp. 107–133, ISBN 978-1-5225-3290-3.
70. Yang, B.; Xiong, Y.; Ma, K.; Liu, S.; Tao, X. Recent Advances in Wearable Textile-based Triboelectric Generator Systems for Energy Harvesting from Human Motion. *EcoMat* **2020**, *2*, e12054. [\[CrossRef\]](#)
71. Goldsmid, H. Bismuth Telluride and Its Alloys as Materials for Thermoelectric Generation. *Materials* **2014**, *7*, 2577–2592. [\[CrossRef\]](#)
72. Xu, B.; Zhang, J.; Yu, G.; Ma, S.; Wang, Y.; Wang, Y. Thermoelectric Properties of Monolayer  $\text{Sb}_2\text{Te}_3$ . *J. Appl. Phys.* **2018**, *124*, 165104. [\[CrossRef\]](#)
73. Chen, X.; Yang, J.; Wu, T.; Li, L.; Luo, W.; Jiang, W.; Wang, L. Nanostructured Binary Copper Chalcogenides: Synthesis Strategies and Common Applications. *Nanoscale* **2018**, *10*, 15130–15163. [\[CrossRef\]](#)
74. Chen, X.-Q.; Fan, S.-J.; Han, C.; Wu, T.; Wang, L.-J.; Jiang, W.; Dai, W.; Yang, J.-P. Multiscale Architectures Boosting Thermoelectric Performance of Copper Sulfide Compound. *Rare Met.* **2021**, *40*, 2017–2025. [\[CrossRef\]](#)
75. Mulla, R.; Rabinal, M.H.K. Copper Sulfides: Earth-Abundant and Low-Cost Thermoelectric Materials. *Energy Technol.* **2019**, *7*, 1800850. [\[CrossRef\]](#)
76. Dennler, G.; Chmielowski, R.; Jacob, S.; Capet, F.; Roussel, P.; Zastrow, S.; Nielsch, K.; Opahle, I.; Madsen, G.K.H. Are Binary Copper Sulfides/Selenides Really New and Promising Thermoelectric Materials? *Adv. Energy Mater.* **2014**, *4*, 1301581. [\[CrossRef\]](#)
77. Lund, A.; Tian, Y.; Darabi, S.; Müller, C. A Polymer-Based Textile Thermoelectric Generator for Wearable Energy Harvesting. *J. Power Sources* **2020**, *480*, 228836. [\[CrossRef\]](#)
78. Rathore, S.S.; Singh, A.; Kumar, P.; Alam, N.; Sahu, M.K.; Sanjay, R. *Review of Exhaust Gas Heat Recovery Mechanism for Internal Combustion Engine Using Thermoelectric Principle*; SAE Technical Paper No. 2018-01-1363; SAE: Warrendale, PA, USA, 2018.
79. Kim, Y.; Lund, A.; Noh, H.; Hofmann, A.I.; Craighero, M.; Darabi, S.; Zokaei, S.; Park, J.I.; Yoon, M.; Müller, C. Robust PEDOT:PSS Wet-Spun Fibers for Thermoelectric Textiles. *Macromol. Mater. Eng.* **2020**, *305*, 1900749. [\[CrossRef\]](#)
80. Zhu, S.; Fan, Z.; Feng, B.; Shi, R.; Jiang, Z.; Peng, Y.; Gao, J.; Miao, L.; Koumoto, K. Review on Wearable Thermoelectric Generators: From Devices to Applications. *Energies* **2022**, *15*, 3375. [\[CrossRef\]](#)
81. Jaziri, N.; Boughamoura, A.; Müller, J.; Mezghani, B.; Tounsi, F.; Ismail, M. A Comprehensive Review of Thermoelectric Generators: Technologies and Common Applications. *Energy Rep.* **2020**, *6*, 264–287. [\[CrossRef\]](#)
82. Kanaujia, B.K.; Singh, N.; Kumar, S. *Rectenna: Wireless Energy Harvesting System, Advances in Sustainability Science and Technology*; Springer: Singapore, 2021; ISBN 9789811625350.
83. Ibrahim, H.H.; Singh, M.J.; Al-Bawri, S.S.; Ibrahim, S.K.; Islam, M.T.; Alzamil, A.; Islam, M.S. Radio Frequency Energy Harvesting Technologies: A Comprehensive Review on Designing, Methodologies, and Potential Applications. *Sensors* **2022**, *22*, 4144. [\[CrossRef\]](#)
84. Vital, D.; Bhardwaj, S.; Volakis, J.L. Textile-Based Large Area RF-Power Harvesting System for Wearable Applications. *IEEE Trans. Antennas Propag.* **2020**, *68*, 2323–2331. [\[CrossRef\]](#)
85. Brown, W.C. The History of Wireless Power Transmission. *Sol. Energy* **1996**, *56*, 3–21. [\[CrossRef\]](#)
86. Javaid, E.M.A.; Bhatti, D.K.L.; Raza, E.Z.; Ilyas, E.U. Wireless Power Transmission “A Potential Idea for Future”. *Int. J. Sci. Eng. Res.* **2015**, *6*, 6.
87. Donchev, E.; Pang, J.S.; Gammon, P.M.; Centeno, A.; Xie, F.; Petrov, P.K.; Breeze, J.D.; Ryan, M.P.; Riley, D.J.; McN, N. The Rectenna Device: From Theory to Practice (a Review). *MRS Energy Sustain.* **2014**, *1*, 1. [\[CrossRef\]](#)
88. Massey, P.J. Mobile Phone Fabric Antennas Integrated within Clothing. *IET* **2001**, *1*, 344–347.
89. Vallozzi, L.; Hertleer, C.; Rogier, H. Latest Developments in the Field of Textile Antennas. In *Smart Textiles and Their Applications*; Koncar, V., Ed.; Elsevier: Amsterdam, The Netherlands, 2016; pp. 599–626, ISBN 978-0-08-100574-3.
90. Brown, W.C. *The History of the Development of the Rectenna*; NASA: Houston, TX, USA, 1980; p. 10.
91. Wireless Power Transmission. *Design and Optimization of Passive UHF RFID Systems*; Curty, J.-P., Declercq, M., Dehollain, C., Joehl, N., Eds.; Springer: Boston, MA, USA, 2007; pp. 3–15, ISBN 978-0-387-44710-0.
92. Saleem, H. Review of Various Aspects of Radio Frequency Identification (RFID) Technology. *IOSR J. Comput. Eng.* **2012**, *8*, 6. [\[CrossRef\]](#)
93. Cardullo, M.; Parks, W. Transponder Apparatus and System. U.S. Patent 3713148A, 23 January 1973.

94. Susnea, I.; Vasiliu, G. On Using Passive RFID Tags to Control Robots for Path Following. *Stud. Inform. Control* **2011**, *20*, 157–162. [\[CrossRef\]](#)
95. Gupta, B.B.; Quamara, M. A Taxonomy of Various Attacks on Smart Card-Based Applications and Countermeasures. *Concurr. Comput. Pract. Exp.* **2021**, *33*, 1. [\[CrossRef\]](#)
96. Guthery, S.B. Java Card: Internet Computing on a Smart Card. *IEEE Internet Comput.* **1997**, *1*, 57–59. [\[CrossRef\]](#)
97. Mou, X.; Sun, H. Wireless Power Transfer: Survey and Roadmap. In Proceedings of the 2015 IEEE 81st Vehicular Technology Conference (VTC Spring), Glasgow, UK, 11–14 May 2015; pp. 1–5.
98. Li, S.; Mi, C.C. Wireless Power Transfer for Electric Vehicle Applications. *IEEE J. Emerg. Sel. Top. Power Electron.* **2015**, *3*, 4–17. [\[CrossRef\]](#)
99. Triviño, A.; González-González, J.M.; Aguado, J.A. Wireless Power Transfer Technologies Applied to Electric Vehicles: A Review. *Energies* **2021**, *14*, 1547. [\[CrossRef\]](#)
100. Mahesh, A.; Chokkalingam, B.; Mihet-Popa, L. Inductive Wireless Power Transfer Charging for Electric Vehicles—A Review. *IEEE Access* **2021**, *9*, 137667–137713. [\[CrossRef\]](#)
101. Haerinia, M.; Shadid, R. Wireless Power Transfer Approaches for Medical Implants: A Review. *Signals* **2020**, *1*, 209–229. [\[CrossRef\]](#)
102. Locher, I.; Klemm, M.; Kirstein, T.; Trster, G. Design and Characterization of Purely Textile Patch Antennas. *IEEE Trans. Adv. Packag.* **2006**, *29*, 777–788. [\[CrossRef\]](#)
103. Salonen, P.; Hurme, L. A Novel Fabric WLAN Antenna for Wearable Applications. In Proceedings of the IEEE Antennas and Propagation Society International Symposium. Digest. Held in Conjunction with: USNC/CNC/URSI North American Radio Sci. Meeting (Cat. No.03CH37450), Columbus, OH, USA, 22–27 June 2003; Volume 2, pp. 700–703.
104. Salonen, P.; Rahmat-Samii, Y.; Hurme, H.; Kivikoski, M. Dual-Band Wearable Textile Antenna. In Proceedings of the IEEE Antennas and Propagation Society Symposium, Monterey, CA, USA, 20–25 June 2004; IEEE: Monterey, CA, USA, 2004; Volume 1, pp. 463–466.
105. Klemm, M.; Locher, I.; Troster, G. A Novel Circularly Polarized Textile Antenna for Wearable Applications. *Eur. Conf. Wirel. Technol.* **2004**, *4*, 285–288.
106. Mukai, Y.; Suh, M. Design and Characterization of a Cotton Fabric Antenna for On-Body Thermotherapy. *J. Ind. Text.* **2022**, *51*, 1627S–1644S. [\[CrossRef\]](#)
107. Salvado, R.; Loss, C.; Gonçalves, R.; Pinho, P. Textile Materials for the Design of Wearable Antennas: A Survey. *Sensors* **2012**, *12*, 15841–15857. [\[CrossRef\]](#)
108. Mukai, Y.; Bharambe, V.T.; Adams, J.J.; Suh, M. Effect of Bending and Padding on the Electromagnetic Performance of a Laser-Cut Fabric Patch Antenna. *Text. Res. J.* **2019**, *89*, 2789–2801. [\[CrossRef\]](#)
109. Mukai, Y.; Bharambe, V.T.; Adams, J.J.; Suh, M. Effect of Bending and Padding on the Electromagnetic Performance of a Laser-Cut Woven Fabric Patch Antenna. In Proceedings of the Textiles Research Open House, Raleigh, NC, USA, 16 April 2018.
110. Johnson, M.; Patel, H.; Tikoo, P.; D’britto, J. Survey on Antennas and Their Types. *Int. J. Sci. Technol. Eng.* **2017**, *3*, 9.
111. Carr, J.J.; Hippisley, G. *Practical Antenna Handbook*, 5th ed.; McGraw-Hill/TAB Electronics: New York, NY, USA, 2012; ISBN 978-0-07-163959-0.
112. Nguyen, S.H.; Ellis, N.; Amirtharajah, R. Powering Smart Jewelry Using an RF Energy Harvesting Necklace. In Proceedings of the 2016 IEEE MTT-S International Microwave Symposium (IMS), San Francisco, CA, USA, 22–27 May 2016; pp. 1–4.
113. Ullah, A.; Keshavarz, R.; Abolhasan, M.; Lipman, J.; Esselle, K.P.; Shariati, N. A Review on Antenna Technologies for Ambient RF Energy Harvesting and Wireless Power Transfer: Designs, Challenges and Applications. *IEEE Access* **2022**, *10*, 17231–17267. [\[CrossRef\]](#)
114. Balanis, C.A. *Antenna Theory: Analysis and Design*, 4th ed.; Wiley: Hoboken, NJ, USA, 2016.
115. Zhang, G.; Li, C.; Zhang, X.; Zhang, J.; Chen, L.; Liu, F. Optimized Sleeve Monopole Antenna for Detection of Electrostatic Discharge Radiation of Spacecraft Solar Array. *Rev. Sci. Instrum.* **2019**, *90*, 015008. [\[CrossRef\]](#)
116. Losito, O.; Dimiccoli, V. Travelling Planar Wave Antenna for Wireless Communications. In *Wireless Communications and Networks—Recent Advances*; Eksim, A., Ed.; InTech: Rijeka, Croatia, 2012; ISBN 978-953-51-0189-5.
117. Alex-Amor, A.; Palomares-Caballero, Á.; Fernández-González, J.M.; Padilla, P.; Marcos, D.; Sierra-Castañer, M.; Esteban, J. RF Energy Harvesting System Based on an Archimedean Spiral Antenna for Low-Power Sensor Applications. *Sensors* **2019**, *19*, 1318. [\[CrossRef\]](#)
118. Ma, Q.; Ray, L.; Haider, M.R. A Miniaturized Spiral Antenna for Energy Harvesting of Implantable Medical Devices. In Proceedings of the 8th International Conference on Electrical and Computer Engineering, Dhaka, Bangladesh, 20–22 December 2014; pp. 180–183.
119. Roy, S.; Tiang, J.J.; Roslee, M.B.; Ahmed, M.T.; Kouzani, A.Z.; Mahmud, M.A.P. Quad-Band Rectenna for Ambient Radio Frequency (RF) Energy Harvesting. *Sensors* **2021**, *21*, 7838. [\[CrossRef\]](#)
120. Song, C.; Huang, Y.; Carter, P.; Zhou, J.; Yuan, S.; Xu, Q.; Kod, M. A Novel Six-Band Dual CP Rectenna Using Improved Impedance Matching Technique for Ambient RF Energy Harvesting. *IEEE Trans. Antennas Propag.* **2016**, *64*, 3160–3171. [\[CrossRef\]](#)
121. Ren, R.; Huang, J.; Sun, H. Investigation of Rectenna’s Bandwidth for RF Energy Harvesting. In Proceedings of the 2020 IEEE MTT-S International Microwave Workshop Series on Advanced Materials and Processes for RF and THz Applications (IMWS-AMP), Suzhou, China, 29–31 July 2020; pp. 1–2.



122. González, F.J.; Boreman, G.D. Comparison of Dipole, Bowtie, Spiral and Log-Periodic IR Antennas. *Infrared Phys. Technol.* **2005**, *46*, 418–428. [\[CrossRef\]](#)
123. Nagarjun, R.; George, G.; Thiripurasundari, D.; Poonkuzhali, R.; Alex, Z.C. Design of a Triple Band Planar Bow-Tie Antenna for Wearable Applications. In Proceedings of the 2013 IEEE Conference on Information and Communication Technologies, Thuckalay, India, 11–12 April 2013; pp. 1185–1189.
124. Kwiatkowski, E.; Estrada, J.A.; López-Yela, A.; Popović, Z. Broadband RF Energy-Harvesting Arrays. *Proc. IEEE* **2022**, *110*, 74–88. [\[CrossRef\]](#)
125. El-Nady, S.; Zamel, H.; Hendy, M.; Attiya, A.; Zekry, A. Performance Enhancement of End-Fire Bow-Tie Antenna by Using Zero Index Metamaterial. In Proceedings of the 2017 Progress in Electromagnetics Research Symposium—Fall (PIERS—FALL), Singapore, 19–22 November 2017; pp. 1895–1900.
126. Kenyon, C.; Fazi, C. *Analysis of a UHF Log-Periodic Antenna*; Defense Technical Information Center: Fort Belvoir, VA, USA, 2012.
127. Dubrovka, F.F.; Lytvyn, M.M.; Lytvyn, S.M.; Martynyuk, S.Y.; Ryabkin, Y.V.; Vtorov, O.O. Ultrawideband Log-Periodic Dipole Antenna Arrays for the Frequency Range 0.7–12 GHz. In Proceedings of the 2005 5th International Conference on Antenna Theory and Techniques, Kyiv, Ukraine, 24–27 May 2005; pp. 110–115.
128. Malisuwan, S.; Tiamnara, N.; Suriyakrai, N. Design of Antennas for a Rectenna System of Wireless Power Transfer in the LTE/WLAN Frequency Band. *J. Clean Energy Technol.* **2017**, *5*, 42–46. [\[CrossRef\]](#)
129. Shrestha, S.; Noh, S.-K.; Choi, D.-Y. Comparative Study of Antenna Designs for RF Energy Harvesting. *Int. J. Antennas Propag.* **2013**, *2013*, 385260. [\[CrossRef\]](#)
130. Mrnka, M.; Vasina, P.; Kufa, M.; Hebelka, V.; Raida, Z. The RF Energy Harvesting Antennas Operating in Commercially Deployed Frequency Bands: A Comparative Study. *Int. J. Antennas Propag.* **2016**, *2016*, 7379624. [\[CrossRef\]](#)
131. Seimeni, M.A.; Tsois, A.; Alexandridis, A.A.; Pantelopoulou, S.A. Mitigation of End-User's Exposure to EMF of Wearable Antennas through Ground-Plane Interventions. In Proceedings of the Loughborough Antennas & Propagation Conference (LAPC 2018), Loughborough, UK, 12–13 November 2018; pp. 99–104.
132. Seimeni, M.A.; Tsois, A.; Alexandridis, A.A.; Pantelopoulou, S.A. Human Exposure to EMFs from Wearable Textile Patch Antennas: Experimental Evaluation of the Ground-Plane Effect. *Prog. Electromagn. Res. B* **2021**, *92*, 71–89. [\[CrossRef\]](#)
133. Balanis, C.A. *Advanced Engineering Electromagnetics*, 2nd ed.; Wiley: Hoboken, NJ, USA, 2012; ISBN 978-0-470-58948-9.
134. Bancroft, R. *Microstrip and Printed Antenna Design*, 4th ed.; SciTech Publishing: Raleigh, NC, USA, 2009; ISBN 978-1-61353-115-0.
135. Mukai, Y. Inkjet-Printed Wearable Antennas for Hyperthermia Treatment. Master's Thesis, North Carolina State University, Raleigh, NC, USA, 2016.
136. Wagih, M.; Weddell, A.S.; Beeby, S. Millimeter-Wave Textile Antenna for on-Body RF Energy Harvesting in Future 5G Networks. In Proceedings of the 2019 IEEE Wireless Power Transfer Conference (WPTC), London, UK, 18–21 June 2019; pp. 245–248.
137. Potti, D.; Mohammed, G.N.A.; Savarimuthu, K.; Narendhiran, S.; Rajamanickam, G. An Ultra-wideband Rectenna Using Optically Transparent Vivaldi Antenna for Radio Frequency Energy Harvesting. *Int. J. RF Microw. Comput.-Aided Eng.* **2020**, *30*, e22362. [\[CrossRef\]](#)
138. Kanaya, H.; Tsukamaoto, S.; Hirabaru, T.; Kanemoto, D.; Pokharel, R.K.; Yoshida, K. Energy Harvesting Circuit on a One-Sided Directional Flexible Antenna. *IEEE Microw. Wirel. Compon. Lett.* **2013**, *23*, 164–166. [\[CrossRef\]](#)
139. Palazzi, V.; Kalialakis, C.; Alimenti, F.; Mezzanotte, P.; Roselli, L.; Collado, A.; Georgiadis, A. Performance Analysis of a Ultra-Compact Low-Power Rectenna in Paper Substrate for RF Energy Harvesting. In Proceedings of the 2017 IEEE Topical Conference on Wireless Sensors and Sensor Networks (WiSNet), Phoenix, AZ, USA, 15–18 January 2017; pp. 65–68.
140. Eid, A.; Costantine, J.; Tawk, Y.; Ramadan, A.H.; Abdallah, M.; ElHajj, R.; Awad, R.; Kasbah, I.B. An Efficient RF Energy Harvesting System. In Proceedings of the 2017 11th European Conference on Antennas and Propagation (EUCAP), Paris, France, 19–24 March 2017; pp. 896–899.
141. Li, W.-W.; Qin, Z.-Z.; Chen, S.-J.; Zhang, L.; Liu, Q.-H. A Wideband Printed Slot Antenna with Harmonic Suppression. *Microw. Opt. Technol. Lett.* **2018**, *60*, 1946–1952. [\[CrossRef\]](#)
142. Song, C.; Huang, Y.; Zhou, J.; Carter, P.; Yuan, S.; Xu, Q.; Fei, Z. Matching Network Elimination in Broadband Rectennas for High-Efficiency Wireless Power Transfer and Energy Harvesting. *IEEE Trans. Ind. Electron.* **2017**, *64*, 3950–3961. [\[CrossRef\]](#)
143. Trikolikar, A.; Lahudkar, S. A Review on Different Parameters Considered for Improvement in Power Conversion Efficiency of Rectenna. In *Proceedings of the 2nd International Conference on Communications and Cyber Physical Engineering (ICCCE 2019)*; Kumar, A., Mozar, S., Eds.; Springer: Singapore, 2020; Volume 570, pp. 79–85, ISBN 9789811387142.
144. Pozar, D.M. *Microwave Engineering*, 4th ed.; John Wiley & Sons, Inc.: Hoboken, NJ, USA, 2011; ISBN 978-0-470-63155-3.
145. Necibi, O.; Guesmi, C.; Gharsallah, A. A New 30 GHz AMC/PRS RFID Reader Antenna with Circular Polarization. *Int. J. Adv. Comput. Sci. Appl.* **2017**, *8*, 35–45. [\[CrossRef\]](#)
146. Sharma, S.; Tripathi, C.C.; Rishi, R. Impedance Matching Techniques for Microstrip Patch Antenna. *Indian J. Sci. Technol.* **2017**, *10*, 1–16. [\[CrossRef\]](#)
147. Kusama, Y.; Isozaki, R. Compact and Broadband Microstrip Band-Stop Filters with Single Rectangular Stubs. *Appl. Sci.* **2019**, *9*, 248. [\[CrossRef\]](#)
148. Cansiz, M.; Altinel, D.; Kurt, G.K. Efficiency in RF Energy Harvesting Systems: A Comprehensive Review. *Energy* **2019**, *174*, 292–309. [\[CrossRef\]](#)
149. Wing, A.H.; Eisenstein, J. Single- and Double-Stub Impedance Matching. *J. Appl. Phys.* **1944**, *15*, 615–622. [\[CrossRef\]](#)

150. Arai, H.; Durnan, G.J.; Saito, S. A Dual Element Patch Array Antenna Structure with Microstrip Triple Stub Matching. In Proceedings of the IEEE Antennas and Propagation Society International Symposium. Digest. Held in conjunction with: USNC/CNC/URSI North American Radio Sci. Meeting (Cat. No.03CH37450), Columbus, OH, USA, 22–27 June 2003; Volume 4, pp. 528–531.
151. Silicon Laboratories Inc. *AN1275: Impedance Matching Network Architectures*; Silicon Laboratories Inc.: Austin, TX, USA, 2022.
152. Aravindh Kumar, A.R.; Singh, S.G.; Dutta, A. Analytical Design Technique for Real-to-real Single- and Dual-frequency Impedance Matching Networks in Lossy Passive Environment. *IET Microw. Antennas Propag.* **2018**, *12*, 1013–1020. [\[CrossRef\]](#)
153. Kim, S.; Cho, J.-H.; Hong, S.-K. A Full Wave Voltage Multiplier for RFID Transponders. *IEICE Trans. Commun.* **2008**, *E91-B*, 388–391. [\[CrossRef\]](#)
154. Krishnachaitanya, P.; Pushpalatha, A. RF Energy Harvesting and Wireless Power Transfer. In Proceedings of the 2015 IEEE 15th Mediterranean Microwave Symposium (MMS), Lecce, Italy, 30 November–2 December 2015.
155. Seah, W.K.G.; Tan, Y.K.; Chan, A.T.S. Research in Energy Harvesting Wireless Sensor Networks and the Challenges Ahead. In *Autonomous Sensor Networks, Springer Series on Chemical Sensors and Biosensors*; Filippini, D., Ed.; Springer: Berlin, Germany, 2012; Volume 13, pp. 73–93, ISBN 978-3-642-34647-7.
156. Gao, Y.; Xie, C.; Zheng, Z. Textile Composite Electrodes for Flexible Batteries and Supercapacitors: Opportunities and Challenges. *Adv. Energy Mater.* **2021**, *11*, 2002838. [\[CrossRef\]](#)
157. Ghouri, A.S.; Aslam, R.; Siddiqui, M.S.; Sami, S.K. Recent Progress in Textile-Based Flexible Supercapacitor. *Front. Mater.* **2020**, *7*, 58. [\[CrossRef\]](#)
158. Xue, Q.; Sun, J.; Huang, Y.; Zhu, M.; Pei, Z.; Li, H.; Wang, Y.; Li, N.; Zhang, H.; Zhi, C. Recent Progress on Flexible and Wearable Supercapacitors. *Small* **2017**, *13*, 1701827. [\[CrossRef\]](#) [\[PubMed\]](#)
159. Sun, H.; Zhang, Y.; Zhang, J.; Sun, X.; Peng, H. Energy Harvesting and Storage in 1D Devices. *Nat. Rev. Mater.* **2017**, *2*, 17023. [\[CrossRef\]](#)
160. Rais, N.H.M.; Soh, P.J.; Malek, F.; Ahmad, S.; Hashim, N.B.M.; Hall, P.S. A Review of Wearable Antenna. In Proceedings of the 2009 Loughborough antennas & propagation conference, Loughborough, UK, 16–17 November 2009.
161. Mukai, Y.; Suh, M. Development of a Conformal Woven Fabric Antenna for Wearable Breast Hyperthermia. *Fash. Text.* **2021**, *8*, 7. [\[CrossRef\]](#)
162. Mukai, Y.; Suh, M. Conformal Cotton Antenna for Wearable Thermotherapy. In Proceedings of the Fiber Society's Spring 2019 Conference, Hong Kong, China, 21–23 May 2019.
163. Mukai, Y.; Suh, M. Development of a Conformal Textile Antenna for Thermotherapy. In Proceedings of the Fiber Society's Fall 2018 Technical Meeting and Conference, Davis, CA, USA, 29–31 October 2018.
164. Morton, W.E.; Hearle, J.W.S. *Physical Properties of Textile Fibres*; Woodhead Publishing: Boca Raton, FL, USA, 2008; ISBN 978-1-84569-220-9.
165. Yamada, Y. Dielectric Properties of Textile Materials: Analytical Approximations and Experimental Measurements—A Review. *Textiles* **2022**, *2*, 50–80. [\[CrossRef\]](#)
166. Mukai, Y. Dielectric Properties of Cotton Fabrics and Their Applications. Ph.D. Thesis, North Carolina State University, Raleigh, NC, USA, 2019.
167. Bal, K.; Kothari, V.K. Permittivity of Woven Fabrics: A Comparison of Dielectric Formulas for Air-Fiber Mixture. *IEEE Trans. Dielectr. Electr. Insul.* **2010**, *17*, 881–889. [\[CrossRef\]](#)
168. Mukherjee, P.K.; Das, S. Improved Analysis of the Dielectric Properties of Textile Materials. *J. Text. Inst.* **2021**, *112*, 1890–1895. [\[CrossRef\]](#)
169. Loss, C.; Gonçalves, R.; Pinho, P.; Salvado, R. Influence of Some Structural Parameters on the Dielectric Behavior of Materials for Textile Antennas. *Text. Res. J.* **2018**, *89*, 1131–1143. [\[CrossRef\]](#)
170. Mukai, Y.; Suh, M. Relationships between Structure and Microwave Dielectric Properties in Cotton Fabrics. *Mater. Res. Express* **2020**, *7*, 015105. [\[CrossRef\]](#)
171. Mukai, Y.; Suh, M. Structure-Microwave Dielectric Property Relationship in Cotton Fabrics. In Proceedings of the Techtextil North America 2019, Raleigh, NC, USA, 26–28 February 2019.
172. Jiyong, H.; Hongyan, J.; Huating, T.; Huan, B.; Hong, H.; Yaya, Z.; Xudong, Y. Influence of Woven Fabric Specification and Yarn Constitutions on the Dielectric Properties at Ultrahigh Frequency. *Mater. Res. Express* **2017**, *4*, 116308. [\[CrossRef\]](#)
173. Hertleer, C.; Laere, A.V.; Rogier, H.; Langenhove, L.V. Influence of Relative Humidity on Textile Antenna Performance. *Text. Res. J.* **2010**, *80*, 177–183. [\[CrossRef\]](#)
174. Lin, C.-H.; Chiu, C.-W.; Gong, J.-Y. A Wearable Rectenna to Harvest Low-Power RF Energy for Wireless Healthcare Applications. In Proceedings of the 2018 11th International Congress on Image and Signal Processing, BioMedical Engineering and Informatics (CISP-BMEI), Beijing, China, 13–15 October 2018.
175. Kuang, Y.; Yao, L.; Luan, H.; Yu, S.; Zhang, R.; Qiu, Y. Effects of Weaving Structures and Parameters on the Radiation Properties of Three-Dimensional Fabric Integrated Microstrip Antennas. *Text. Res. J.* **2017**, *88*, 2182–2189. [\[CrossRef\]](#)
176. Xu, F.; Zhu, H.; Ma, Y.; Qiu, Y. Electromagnetic Performance of a Three-Dimensional Woven Fabric Antenna Conformal with Cylindrical Surfaces. *Text. Res. J.* **2017**, *87*, 147–154. [\[CrossRef\]](#)

177. Obrzut, J.; Emiroglu, C.D.; Pazmino, B.A.; Douglas, J.F.; Gilman, J.W. Characterization of Dielectric Properties and Moisture Uptake of Cellulose Nanocrystals Using Non-Contact Microwave Cavity. In Proceedings of the 2016 International Conference on Nanotechnology and Renewable Materials, Grenoble, France, 13–16 June 2016.
178. Lebaudy, P.; Estel, L.; Ledoux, A. Microwave Heating of Poly(Ethylene Terephthalate) Bottle Preforms Used in the Thermoforming Process. *J. Appl. Polym. Sci.* **2008**, *108*, 2408–2414. [\[CrossRef\]](#)
179. Azlan, A.A.; Badrun, M.K.A.B.H.; Ali, M.T.; Awang, Z.; Saad, Z.B.; Awang, A.H.B. A Comparative Study of Material Leucaena Leucocephala Stem Wood Plastic Composite (WPC) Substrate with FR4 Substrate throughout Single Patch Antenna Design. *Prog. Electromagn. Res. B* **2014**, *59*, 151–166. [\[CrossRef\]](#)
180. Rogers Corporation. RT/Duroid® 5870 /5880 High Frequency Laminates. Available online: <https://rogerscorp.com/-/media/project/rogerscorp/documents/advanced-electronics-solutions/english/data-sheets/rt-duroid-5870---5880-data-sheet.pdf> (accessed on 11 August 2022).
181. Atalie, D.; Gideon, R.K.; Ferede, A.; Tesinova, P.; Lenfeldova, I. Tactile Comfort and Low-Stress Mechanical Properties of Half-Bleached Knitted Fabrics Made from Cotton Yarns with Different Parameters. *J. Nat. Fibers* **2021**, *18*, 1699–1711. [\[CrossRef\]](#)
182. Wang, H.; Memon, H. (Eds.) *Cotton Science and Processing Technology: Gene, Ginning, Garment and Green Recycling*; Springer: Singapore, 2020; ISBN 9789811591686.
183. Thangaselvi, E.; Jeyanthi, K.M.A. Implementation of Flexible Denim Nickel Copper Rip Stop Textile Antenna for Medical Application. *Clust. Comput.* **2019**, *22*, 635–645. [\[CrossRef\]](#)
184. Wagih, M.; Hilton, G.S.; Weddell, A.S.; Beeby, S. 5G-Enabled E-Textiles Based on a Low-Profile Millimeter-Wave Textile Antenna. *Eng. Proc.* **2022**, *15*, 13.
185. Stoppa, M.; Chiolerio, A. Wearable Electronics and Smart Textiles: A Critical Review. *Sensors* **2014**, *14*, 11957–11992. [\[CrossRef\]](#)
186. Varnaitė-Žuravliova, S.; Kavaliauskienė, L.; Baltušnikaitė, J.; Valasevičiūtė, L.; Verbienė, R. Investigation of Shielding Properties of Yarns, Twisted with Metal Wire. *Mater. Sci.* **2014**, *20*, 73–78. [\[CrossRef\]](#)
187. Mikulić, D.; Šopp, E.; Bonefačić, D.; Šipuš, Z. Textile Slotted Waveguide Antennas for Body-Centric Applications. *Sensors* **2022**, *22*, 1046. [\[CrossRef\]](#) [\[PubMed\]](#)
188. Ahmad, S.; Subhani, K.; Rasheed, A.; Ashraf, M.; Afzal, A.; Ramzan, B.; Sarwar, Z. Development of Conductive Fabrics by Using Silver Nanoparticles for Electronic Applications. *J. Electron. Mater.* **2020**, *49*, 1330–1337. [\[CrossRef\]](#)
189. Hu, L.; Pasta, M.; La Mantia, F.; Cui, L.; Jeong, S.; Deshazer, H.D.; Choi, J.W.; Han, S.M.; Cui, Y. Stretchable, Porous, and Conductive Energy Textiles. *Nano Lett.* **2010**, *10*, 708–714. [\[CrossRef\]](#)
190. Yang, X.; Shang, S.; Li, L.; Tao, X.-M.; Yan, F. Vapor Phase Polymerization of 3,4-Ethylenedioxythiophene on Flexible Substrate and Its Application on Heat Generation. *Polym. Adv. Technol.* **2011**, *22*, 1049–1055. [\[CrossRef\]](#)
191. Kazani, I.; Hertleer, C.; De Mey, G.; Guxho, G.; Van Langenhove, L. Dry Cleaning of Electroconductive Layers Screen Printed on Flexible Substrates. *Text. Res. J.* **2013**, *83*, 1541–1548. [\[CrossRef\]](#)
192. Shahariar, H.; Soewardiman, H.; Muchler, C.; Adams, J.; Jur, J. Porous Textile Antenna Designs for Improved Wearability. *Smart Mater. Struct.* **2018**, *27*, 045008. [\[CrossRef\]](#)
193. Singh, R.K.; Michel, A.; Nepa, P.; Salvatore, A. Wearable Dual-Band Quasi-Yagi Antenna for UHF-RFID and 2.4 GHz Applications. *IEEE J. Radio Freq. Identif.* **2020**, *4*, 420–427. [\[CrossRef\]](#)
194. Haynes, W.M. *CRC Handbook of Chemistry and Physics*; CRC Press: Boca Raton, FL, USA, 2016; ISBN 978-1-4987-5429-3.
195. Shirakawa, H.; Louis, E.J.; MacDiarmid, A.G.; Chiang, C.K.; Heeger, A.J. Synthesis of Electrically Conducting Organic Polymers: Halogen Derivatives of Polyacetylene, (CH)<sub>x</sub>. *J. Chem. Soc. Chem. Commun.* **1977**, *16*, 578–580. [\[CrossRef\]](#)
196. Singha, K.; Kumar, J.; Pandit, P. Recent Advancements in Wearable & Smart Textiles: An Overview. *Mater. Today Proc.* **2019**, *16*, 1518–1523. [\[CrossRef\]](#)
197. Mirabedini, A.; Foroughi, J.; Wallace, G.G. Developments in Conducting Polymer Fibres: From Established Spinning Methods toward Advanced Applications. *RSC Adv.* **2016**, *6*, 44687–44716. [\[CrossRef\]](#)
198. Grancarić, A.M.; Jerković, I.; Koncar, V.; Cochrane, C.; Kelly, F.M.; Soulat, D.; Legrand, X. Conductive Polymers for Smart Textile Applications. *J. Ind. Text.* **2018**, *48*, 612–642. [\[CrossRef\]](#)
199. Xu, R.; Wei, J.; Guo, F.; Cui, X.; Zhang, T.; Zhu, H.; Wang, K.; Wu, D. Highly Conductive, Twistable and Bendable Polypyrrole-Carbon Nanotube Fiber for Efficient Supercapacitor Electrodes. *RSC Adv.* **2015**, *5*, 22015–22021. [\[CrossRef\]](#)
200. Lepró, X.; Lima, M.D.; Baughman, R.H. Spinnable Carbon Nanotube Forests Grown on Thin, Flexible Metallic Substrates. *Carbon* **2010**, *48*, 3621–3627. [\[CrossRef\]](#)
201. Sengupta, J. Carbon Nanotube Fabrication at Industrial Scale. In *Handbook of Nanomaterials for Industrial Applications*; Hussain, C.M., Ed.; Elsevier: Amsterdam, The Netherlands, 2018; pp. 172–194, ISBN 978-0-12-813351-4.
202. Al-Maqdasi, Z.; Hajlane, A.; Renbi, A.; Ouarga, A.; Chouhan, S.S.; Joffe, R. Conductive Regenerated Cellulose Fibers by Electroless Plating. *Fibers* **2019**, *7*, 38. [\[CrossRef\]](#)
203. Yu, D.; Mu, S.; Liu, L.; Wang, W. Preparation of Electroless Silver Plating on Aramid Fiber with Good Conductivity and Adhesion Strength. *Colloids Surf. Physicochem. Eng. Asp.* **2015**, *483*, 53–59. [\[CrossRef\]](#)
204. Kirstein, T. *Multidisciplinary Know-How for Smart-Textiles Developers*; Woodhead Publishing Limited: Cambridge, UK, 2013; ISBN 978-0-85709-342-4.



205. Schwarz, A.; Hakuzimana, J.; Gasana, E.; Westbroek, P.; Van Langenhove, L. Gold Coated Polyester Yarn. In Proceedings of the 3rd International Conference on Smart Materials, Structures and Systems, Sicily, Italy, 8–13 June 2008; pp. 47–51.
206. Xu, F.; Zhang, K.; Qiu, Y. Light-Weight, High-Gain Three-Dimensional Textile Structural Composite Antenna. *Compos. Part B Eng.* **2020**, *185*, 107781. [[CrossRef](#)]
207. Choudhry, N.A.; Shekhar, R.; Rasheed, A.; Arnold, L.; Wang, L. Effect of Conductive Thread and Stitching Parameters on the Sensing Performance of Stitch-Based Pressure Sensors for Smart Textile Applications. *IEEE Sens. J.* **2022**, *22*, 6353–6363. [[CrossRef](#)]
208. Ruppert-Stroescu, M.; Balasubramanian, M. Effects of Stitch Classes on the Electrical Properties of Conductive Threads. *Text. Res. J.* **2018**, *88*, 2454–2463. [[CrossRef](#)]
209. Kiourti, A. Textile-Based Flexible Electronics for Wearable Applications: From Antennas to Batteries. In Proceedings of the 2018 2nd URSI Atlantic Radio Science Meeting (AT-RASC), Gran Canaria, Spain, 28 May–1 June 2018.
210. Chaudhari, S.; Alharbi, S.; Zou, C.; Shah, H.; Harne, R.L.; Kiourti, A. A New Class of Reconfigurable Origami Antennas Based on E-Textile Embroidery. In Proceedings of the 2018 IEEE International Symposium on Antennas and Propagation & USNC/URSI National Radio Science Meeting, Boston, MA, USA, 8–13 July 2018; pp. 183–184.
211. Alharbi, S.; Chaudhari, S.; Inshaar, A.; Shah, H.; Zou, C.; Harne, R.L.; Kiourti, A. E-Textile Origami Dipole Antennas with Graded Embroidery for Adaptive RF Performance. *IEEE Antennas Wirel. Propag. Lett.* **2018**, *17*, 2218–2222. [[CrossRef](#)]
212. Adanur, S. *Handbook of Weaving*; CRC Press: Boca Raton, FL, USA, 2000; ISBN 978-1-58716-013-4.
213. Spencer, D.J. *Knitting Technology: A Comprehensive Handbook and Practical Guide*, 3rd ed.; Woodhead Publishing Limited: Cambridge, UK, 2001; ISBN 978-1-85573-333-6.
214. Kazan, I.; Hertleer, C.; De Mey, G.; Schwarz, A.; Guxho, G.; Van Langenhove, L. Electrical Conductive Textiles Obtained by Screen Printing. *FIBRES Text. East. Eur.* **2012**, *1*, 57–63.
215. Cummins, G.; Desmulliez, M.P.Y. Inkjet Printing of Conductive Materials: A Review. *Circuit World* **2012**, *38*, 193–213. [[CrossRef](#)]
216. Shahariar, H.; Kim, I.; Soewardiman, H.; Jur, J.S. Inkjet Printing of Reactive Silver Ink on Textiles. *ACS Appl. Mater. Interfaces* **2019**, *11*, 6208–6216. [[CrossRef](#)] [[PubMed](#)]
217. Yao, L.; Qiu, Y. Design and Electromagnetic Properties of Conformal Single-Patch Microstrip Antennas Integrated into Three-Dimensional Orthogonal Woven Fabrics. *Text. Res. J.* **2015**, *85*, 561–567. [[CrossRef](#)]
218. Xu, F.; Yao, L.; Zhao, D.; Jiang, M.; Qiu, Y. Effect of Weaving Direction of Conductive Yarns on Electromagnetic Performance of 3D Integrated Microstrip Antenna. *Appl. Compos. Mater.* **2013**, *20*, 827–838. [[CrossRef](#)]
219. Zhang, S.; Chauraya, A.; Seager, R.; Vardaxoglou, Y.C.; Whittow, W.; Acti, T.; Dias, T. Fully Fabric Knitted Antennas for Wearable Electronics. In Proceedings of the 2013 USNC-URSI Radio Science Meeting (Joint with AP-S Symposium), Lake Buena Vista, FL, USA, 7–13 July 2013; p. 215.
220. Song, L.; Zhang, B.; Zhang, D.; Rahmat-Samii, Y. Embroidery Electro-Textile Patch Antenna Modeling and Optimization Strategies with Improved Accuracy and Efficiency. *IEEE Trans. Antennas Propag.* **2022**, *70*, 6388–6400. [[CrossRef](#)]
221. Zhang, S.; Chauraya, A.; Whittow, W.; Seager, R.; Acti, T.; Dias, T.; Vardaxoglou, Y. Repeatability of Embroidered Patch Antennas. In Proceedings of the 2013 Loughborough Antennas & Propagation Conference (LAPC), Loughborough, UK, 11–12 November 2013; pp. 140–144.
222. Zhang, S.; Chauraya, A.; Whittow, W.; Seager, R.; Acti, T.; Dias, T.; Vardaxoglou, Y. Embroidered Wearable Antennas Using Conductive Threads with Different Stitch Spacings. In Proceedings of the 2012 Loughborough Antennas Propagation Conference (LAPC), Loughborough, UK, 12–13 November 2012.
223. Kiourti, A.; Volakis, J. Colorful Textile Antennas Integrated into Embroidered Logos. *J. Sens. Actuator Netw.* **2015**, *4*, 371–377. [[CrossRef](#)]
224. Gil, I.; Fernández-García, R.; Tornero, J.A. Embroidery Manufacturing Techniques for Textile Dipole Antenna Applied to Wireless Body Area Network. *Text. Res. J.* **2019**, *89*, 1573–1581. [[CrossRef](#)]
225. Kapetanakis, T.N.; Pavec, M.; Ioannidou, M.P.; Nikolopoulos, C.D.; Baklezos, A.T.; Soukup, R.; Vardiambasis, I.O. Embroidered Bow-Tie Wearable Antenna for the 868 and 915 MHz ISM Bands. *Electronics* **2021**, *10*, 1983. [[CrossRef](#)]
226. Roudjane, M.; Khalil, M.; Miled, A.; Messaddeq, Y. New Generation Wearable Antenna Based on Multimaterial Fiber for Wireless Communication and Real-Time Breath Detection. *Photonics* **2018**, *5*, 33. [[CrossRef](#)]
227. Cupal, M.; Raida, Z. Slot Antennas Integrated into 3D Knitted Fabrics: 5.8 GHz and 24 GHz ISM Bands. *Sensors* **2022**, *22*, 2707. [[CrossRef](#)]
228. Alhawari, A.R.H.; Saeidi, T.; Alkawgani, A.H.M.; Hindi, A.T.; Alghamdi, H.; Alsuwian, T.; Awwad, S.A.B.; Imran, M.A. Wearable Metamaterial Dual-Polarized High Isolation UWB MIMO Vivaldi Antenna for 5G and Satellite Communications. *Micromachines* **2021**, *12*, 1559. [[CrossRef](#)] [[PubMed](#)]
229. Johnson, A.D.; Nichols, M.W.; Venkatakrishnan, S.B.; Volakis, J.L. Reconfigurable Log-Periodic Dipole Array on Textile. *IET Microw. Antennas Propag.* **2020**, *14*, 1791–1794. [[CrossRef](#)]
230. Estrada, J.A.; Kwiatkowski, E.; Lopez-Yela, A.; Borgonos-Garcia, M.; Segovia-Vargas, D.; Barton, T.; Popovic, Z. RF-Harvesting Tightly Coupled Rectenna Array Tee-Shirt with Greater Than Octave Bandwidth. *IEEE Trans. Microw. Theory Tech.* **2020**, *68*, 3908–3919. [[CrossRef](#)]

- 
231. Galoić, A.; Ivsic, B.; Bonefacic, D.; Bartolic, J. Wearable Energy Harvesting Using Wideband Textile Antennas. In Proceedings of the 2016 10th European Conference on Antennas and Propagation (EuCAP), Davos, Switzerland, 10–15 April 2016; pp. 1–5.
  232. Seymour, S. *Fashionable Technology: The Intersection of Design, Fashion, Science, and Technology*; Springer: Vienna, Austria, 2008; ISBN 978-3-211-74498-7.